

1 Adaptive ecological processes and metabolic 2 independence drive microbial colonization and 3 resilience in the human gut

4 Andrea R. Watson^{1,2}, Jessika Füssel², Iva Veseli⁴, Johanna Zaal DeLongchamp³,
5 Marisela Silva³, Florian Trigodet², Karen Lolans², Alon Shaiber⁴, Emily Fogarty^{1,2},
6 Christopher Quince⁵, Michael K. Yu⁶, Arda Söylev⁷, Hilary G. Morrison⁸, Sonny T.M. Lee²,
7 David T. Rubin², Bana Jabri², Thomas Louie³, A. Murat Eren^{1,2,4,8,*}

8 ¹Committee on Microbiology, The University of Chicago, Chicago, IL 60637, USA. ²Department of
9 Medicine, The University of Chicago, Chicago, IL 60637, USA. ³Department of Medicine, The
10 University of Calgary, Calgary, AB T2N 1N4, Canada. ⁴Biophysical Sciences Program, The
11 University of Chicago, Chicago, IL 60637, USA. ⁵Organisms and Ecosystems, Earlham Institute,
12 Norwich, Norwich, NR4 7UZ, United Kingdom. ⁶Toyota Technological Institute at Chicago,
13 Chicago, IL 60637, USA. ⁷Department of Computer Engineering, Konya Food and Agriculture
14 University, Konya, Turkey. ⁸Josephine Bay Paul Center, Marine Biological Laboratory, Woods Hole,
15 MA 02543, USA.

16
17 * Corresponding author: meren@uchicago.edu

18

19

20 **Running Title**

21 Drivers of human gut colonization

22 **Keywords**

23 fecal microbiota transplantation; human gut microbiome; microbial colonization; microbial
24 metabolism; metabolic competency.

25 Abstract

26 A detailed understanding of gut microbial ecology is essential to engineer effective
27 microbial therapeutics and to model microbial community assembly and succession in
28 health and disease. However, establishing generalizable insights into the functional
29 determinants of microbial fitness in the human gut has been a formidable challenge. Here
30 we employ fecal microbiota transplantation (FMT) as an *in natura* experimental model to
31 identify determinants of microbial colonization and resilience. Our long-term sampling
32 strategy and high-resolution multi-omics analyses of FMT donors and recipients reveal
33 adaptive ecological processes as the main driver of microbial colonization outcomes after
34 FMT. We also show that high-fitness donor microbial populations are significantly
35 enriched in metabolic pathways that are responsible for the biosynthesis of nucleotides,
36 essential amino acids, and micronutrients, independent of taxonomy. To determine
37 whether such metabolic competence can explain the microbial ecology of human disease
38 states, we analyzed genomes reconstructed from healthy humans and humans with
39 inflammatory bowel disease (IBD). Our data reveal that such traits are also significantly
40 enriched in microbial genomes recovered from IBD patients, linking presence of superior
41 metabolic competence in bacteria to their expansion in IBD. Overall, these findings
42 suggest that the transfer of gut microbes from a healthy donor to a disrupted recipient
43 environment initiates an environmental filter that selects for populations that can self-
44 sustain. Such ecological processes that select for self-sustenance under stress offer a
45 model to explain why common yet typically rare members of healthy gut environments
46 can become dominant in inflammatory conditions without any need for them to be causally
47 associated with, or contribute to, such disease states.

48

49 Introduction

50 The human gut microbiome is associated with a wide range of diseases and disorders
51 (Almeida et al. 2020; Durack and Lynch 2019; Lynch and Pedersen 2016). However,
52 mechanistic underpinnings of these associations have been difficult to resolve in part due
53 to the diversity of human lifestyles (David et al. 2014) and the limited utility of model
54 systems to make robust causal inferences for microbially mediated human diseases
55 (Walter et al. 2020).

56 Inflammatory bowel disease (IBD), a group of increasingly common intestinal disorders
57 that cause inflammation of the gastrointestinal tract (Baumgart and Carding 2007), has
58 been a model to study human diseases associated with the gut microbiota (Schirmer et
59 al. 2019). The pathogenesis of IBD is attributed in part to the gut microbiome (Plichta et
60 al. 2019), yet the microbial ecology of IBD-associated dysbiosis remains a puzzle. Despite
61 marked changes in gut microbial community composition in IBD (Ott et al. 2004; Sokol
62 and Seksik 2010; Joossens et al. 2011), the microbiota associated with the disease lacks
63 traditional pathogens (Chow, Tang, and Mazmanian 2011), and microbes that are found
64 in IBD typically also occur in healthy individuals (Clooney et al. 2021), which complicates
65 the search for robust functional or taxonomic markers of health and disease states (Lloyd-
66 Price et al. 2019). One of the hallmarks of IBD is reduced microbial diversity during
67 episodes of inflammation, when the gut environment is often dominated by microbes that
68 typically occur in lower abundances prior to inflammation (Vineis et al. 2016). The sudden
69 increase in the relative abundance of microbes that are common to healthy individuals
70 suggests that the harsh conditions of IBD likely act as an ecological filter that prevents
71 the persistence of low-fitness populations. Yet, in the absence of a complete
72 understanding of the functional drivers of microbial colonization in this habitat, critical
73 insights into the metabolic requirements of survival in IBD remains elusive.

74 Understanding the determinants of microbial colonization has been one of the
75 fundamental aims of gut microbial ecology (Costello et al. 2012; Messer et al. 2017). To
76 overcome the difficulties of conducting well-controlled studies with humans, researchers
77 have studied the determinants of microbial colonization of the gut in model systems, such

78 as germ-free mice conventionalized with individual taxa (S. M. Lee et al. 2013) or a
79 consortium of human microbial isolates (Feng et al. 2020). Despite their utility for
80 hypothesis testing, simpler models do not capture the complex ecological interactions
81 fostered by natural systems and thus the insights they yield do not always translate to
82 human gut microbial ecology (Ley et al. 2006; Finucane et al. 2014). Between the
83 extremes of well-controlled but simple mouse models and complex yet uncontrolled
84 human populations, there exists a middleground that provides a window into the microbial
85 ecology of complex human systems through a controlled perturbation: human fecal
86 microbiota transplantation (FMT), the transfer of stool from a donor into a recipient's
87 gastrointestinal tract (Eiseman et al. 1958).

88 FMT complements laboratory models of environmental perturbation by colliding two
89 distinct microbial ecosystems, and thus offers a powerful framework to study fundamental
90 questions of microbial ecology, including the determinants of microbial succession and
91 resilience (Schmidt, Raes, and Bork 2018). Here we use FMT as an *in natura*
92 experimental model to investigate the ecological and functional determinants of
93 successful microbial colonization of the human gut at the level of individual populations.
94 Our findings suggest that adaptive ecological forces are key drivers of colonization
95 outcomes after FMT, reveal taxonomy-independent metabolic determinants of fitness in
96 the human gut, and demonstrate that similar ecological principles determine resilience of
97 microbes in stressful and inflammatory conditions.

98 Results and Discussion

99 Our study includes 109 gut metagenomes (Supplementary Table 1) from two healthy FMT
100 donors (A and B) and 10 FMT recipients (five recipients per donor) who had multiply
101 recurrent *Clostridium difficile* infection (CDI) and received vancomycin for a minimum of
102 10 days to attain resolution of diarrheal illness prior to FMT. On the last day of vancomycin
103 treatment, a baseline fecal sample was collected from each recipient, and their bowel
104 contents were evacuated immediately prior to FMT. Recipients did not take any antibiotics
105 on the day of transplant, or during the post-FMT sampling period (Supplementary Figure
106 1). We also collected 24 Donor A samples over a period of 636 days and 15 Donor B

107 samples over a period of 532 days to establish an understanding of the long-term
108 microbial population dynamics within each donor microbiota. We also collected 5 to 9
109 samples from each recipient up to 336 days post-FMT. Deep sequencing of donor and
110 recipient metagenomes using Illumina paired-end (2x150) technology resulted in a total
111 of 7.7 billion sequences with an average of 71 million reads per metagenome (Figure 1,
112 Supplementary Table 1, Supplementary Table 2). We employed genome-resolved
113 metagenomics, pangenomics, and microbial population genetics for an in-depth
114 characterization of donor and recipient gut microbiota using these data, and we leveraged
115 publicly available gut metagenomes to benchmark our observations.

116 Many but not all donor microbes colonized recipients and persisted 117 long-term

118 We first characterized the taxonomic composition of each donor and recipient sample by
119 aligning metagenomic short reads to reference genomes in the NCBI's RefSeq database
120 (Supplementary Table 2). The phylum-level microbial community composition of both
121 donors reflected those observed in healthy individuals in North America (Human
122 Microbiome Project Consortium 2012): a large representation of Firmicutes and
123 Bacteroidetes, and other taxa with relatively lower relative abundances, including
124 Actinobacteria, Verrucomicrobia, and Proteobacteria (Figure 1, Supplementary Table 2).
125 In contrast, the vast majority of the recipient pre-FMT samples were dominated by
126 Proteobacteria, a phylum that typically undergoes a drastic expansion in individuals
127 treated with vancomycin (Isaac et al. 2017). After the FMT, we observed a dramatic shift
128 in recipient taxonomic profiles (Supplementary Table 2, Supplementary Figure 2), a
129 widely documented hallmark of this procedure (Khoruts et al. 2010; Grehan et al. 2010;
130 Shahinas et al. 2012). Nearly all recipient samples post-FMT were dominated by
131 Bacteroidetes and Firmicutes as well as Actinobacteria and Verrucomicrobia in lower
132 abundances, resembling qualitatively, but not quantitatively, the taxonomic profiles of
133 their donors (Supplementary Table 2). For example, even though the median relative
134 abundance of Bacteroidetes populations were 5% and 17% in donors A and B, their
135 relative abundance in recipients post-FMT increased to 33% and 45%, respectively

136 (Figure 1, Supplementary Table 2). A single genus, *Bacteroides*, made up 76% and 82%
137 of the Bacteroidetes populations in the recipients of Donor A and B, respectively
138 (Supplementary Table 2). The success of the donor *Bacteroides* populations in recipients
139 upon FMT is not surprising given the ubiquity of this genus across human populations
140 throughout the globe (Wexler and Goodman 2017) and the ability of its members to
141 survive substantial levels of stress (Swidsinski et al. 2005; Vineis et al. 2016). This result
142 suggests that FMT outcomes in our dataset are unlikely random, and the study design
143 and resulting dataset offers a framework to study ecological principles of the human gut
144 microbiome.

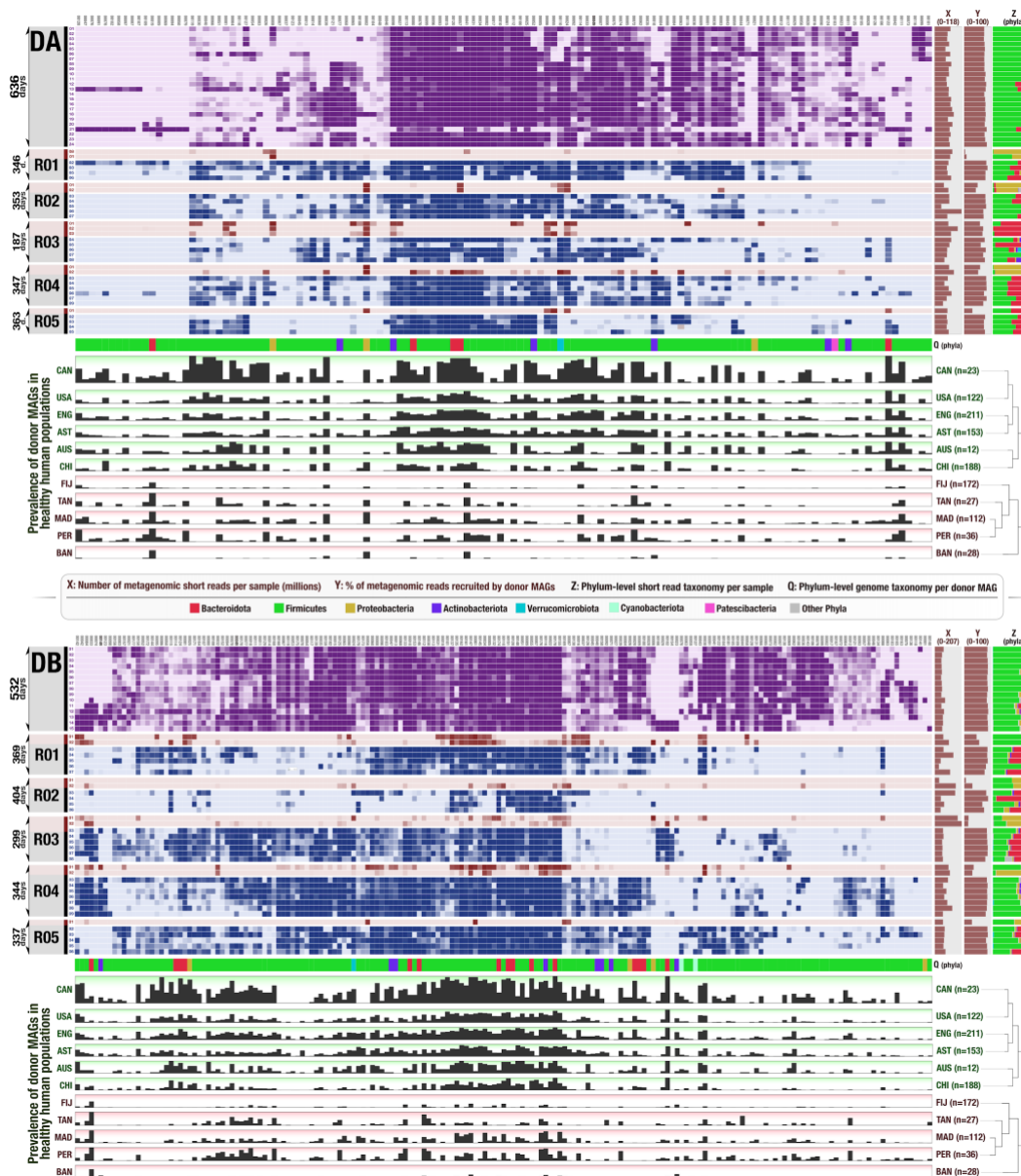
145 Next, we assembled short metagenomic reads into contiguous segments of DNA
146 (contigs). Co-assemblies of 24 Donor A and 15 Donor B metagenomes independently
147 resulted in 53,891 and 54,311 contigs that were longer than 2,500 nucleotides, and
148 described 0.70 and 0.79 million genes occurring in 179 and 248 genomes, as estimated
149 by the mode of the frequency of bacterial single-copy core genes (Supplementary Table
150 2). One way to characterize how well a given assembly describes the DNA content of a
151 given metagenome is to calculate the percentage of reads it recruits from the
152 metagenome through read mapping. Donor contigs recruited on average 80.8% of
153 metagenomic reads from donor metagenomes. In contrast, they recruited 43.4% of reads
154 on average from pre-FMT recipient metagenomes. This number increased to 80.2% for
155 recipient metagenomes post-FMT (Figure 1), and the donor contigs continued to
156 represent 76.8% of the recipient metagenomes on average even after a year post-FMT
157 (Supplementary Table 2). These read recruitment results suggest that members of the
158 donor microbiota successfully established in recipient guts upon FMT and largely
159 persisted until the end of the sampling period.

160 Compared to metagenomic short reads, assembled contigs provide a larger genetic
161 context to study microbial metagenomes. However, a sole focus on contigs may yield
162 misleading results (Kowarsky et al. 2017) that can be ameliorated by reconstructing
163 microbial genomes from metagenomic assemblies (Chen et al. 2020). We reconstructed
164 genomes from co-assembled donor metagenomes by grouping contigs into putative bins
165 based on sequence composition and differential coverage signal as previously described

166 (Sharon et al. 2013; S. T. M. Lee et al. 2017). We retained bins that were at least 70%
167 complete and had no more than 10% redundancy as predicted by bacterial single-copy
168 core genes (Bowers et al. 2017; Chen et al. 2020) and manually refined them to improve
169 their quality following previously described approaches (Delmont et al. 2018; Shaiber et
170 al. 2020). Our binning resulted in a final list of 128 metagenome-assembled genomes
171 (MAGs) for Donor A and 183 MAGs for Donor B that included members of Firmicutes
172 (n=265), Bacteroidetes (n=20), Actinobacteria (n=14), Proteobacteria (n=7),
173 Verrucomicrobia (n=2), Cyanobacteria (n=2), and Patescibacteria (n=1) (Supplementary
174 Table 3). The taxonomy of donor-derived genomes largely reflected the taxonomic
175 composition of donor metagenomes as predicted by short reads (Figure 1,
176 Supplementary Table 2, Supplementary Table 3). While only 20 genomes (mostly of
177 *Bacteroides* and *Alistipes*) explained the entirety of the Bacteroidetes group, we
178 recovered 265 MAGs that represented lower abundance but diverse populations of
179 Firmicutes (Figure 1, Supplementary Table 2, Supplementary Table 3). We found no
180 difference between the delivery method of FMT for the recipients of donor A, where, on
181 average 45% and 43% of donor genomes emerged in recipients who received donor stool
182 through colonoscopy (n=3) versus pills (n=2), respectively. However, there was an
183 increase in the efficiency of pills for donor B, where on average 25% and 54% of donor
184 genomes emerged in recipients who received donor stool through colonoscopy (n=2)
185 versus pill (n=3) (Supplementary Figure 3).

186 Reconstructing genomes gave us access to microbial populations in metagenomes
187 through metagenomic read recruitment strategies and enabled us to characterize (1)
188 population-level microbial colonization dynamics before and after FMT using donor and
189 recipient metagenomes and (2) the distribution of each donor population across
190 geographically distributed humans using 1,984 publicly available human gut
191 metagenomes (Supplementary Table 4). As expected, we detected each donor
192 population in at least one donor metagenome (see Methods for 'detection' criteria). Yet,
193 only 16% of Donor A populations were detected in every Donor A sample, and only 44%
194 of Donor B MAGs were detected in every Donor B sample (Figure 1, Supplementary Table
195 3), in agreement with the previously documented dynamism of gut microbial community
196 composition over time (David et al. 2014). A marked increase in the detection of donor

197 populations in recipients after FMT echoed the general pattern of transfer suggested by
198 the short-read taxonomy (Figure 1): while only 38% of Donor A and 54% of Donor B
199 populations were detected in at least one recipient pre-FMT, these percentages increased
200 to 96% and 96% post-FMT (Supplementary Table 3). Not every donor population
201 colonized each recipient, but colonization events did not appear to be random: while some
202 donor populations colonized all recipients, others colonized none (Figure 1), providing us
203 with an opportunity to resolve colonization events and quantify colonization success for
204 each donor population in our dataset.



206 **Figure 1. FMT Donor genomes across recipients and publicly available gut metagenomes.** In both heat maps
207 each column represents a donor genome and each row represents a metagenome, and each data point represents the
208 detection of a given genome in a given metagenome. Purple rows represent donor metagenomes which cover 636
209 days for Donor A and 532 days for Donor B. Each recipient metagenome is colored red for pre-FMT samples and blue
210 for post-FMT samples. The three rightmost columns display for each metagenome (X) the number of metagenomic
211 short reads in millions, (Y) the percent of metagenomic short reads recruited by genomes, and (Z) the taxonomic
212 composition of metagenomes (based on metagenomic short reads) at the phylum level. The row Q provides the phylum-
213 level taxonomy for each donor genome. Finally, the 11 bottom rows under each heat map show the fraction of healthy
214 adult metagenomes from 11 different countries in which a given donor genome is detected (if a genome is detected in
215 every individual from a country it is represented with a full bar). The dendrograms on the right-hand side of these layers
216 organize countries based on the detection patterns of genomes (Euclidean distance and Ward clustering). Red and
217 green shades represent the two main clusters that emerge from this analysis, where green layers are industrialized
218 countries in which donor genomes are highly prevalent and red layers are less industrialized countries where the
219 prevalence of donor genomes is low.

220 Resolving colonization events accurately is a challenging task as multiple factors may
221 influence the ability to determine colonization outcomes unambiguously. These factors
222 include (1) the inability to detect low-abundance populations, (2) inaccurate
223 characterization of transient populations observed immediately after FMT as successful
224 colonization events, (3) the reliance on relative abundance of populations to define
225 colonization events when abundance estimates from stool do not always reflect the
226 abundance of organisms in the GI tract (Yasuda et al. 2015; Sheth et al. 2019), and (4)
227 the failure to distinguish between colonization by a donor population or emergence of a
228 pre-FMT recipient population after FMT (where a low-abundance recipient population that
229 is closely related to one or more donor populations becomes abundant after FMT and is
230 mistaken as a bona fide colonization event). To mitigate these factors, we have (1)
231 employed deep-sequencing of our metagenomes which averaged 71 million reads per
232 sample, (2) implemented a longitudinal sampling strategy, that spanned 376 days on
233 average, to observe donor populations in our recipients long after the FMT, (3) leveraged
234 a ‘detection’ metric to define colonization events by presence/absence of populations
235 rather than abundance, and (4) employed microbial population genetics to identify and
236 resolve origins of subpopulations. We also developed an analytical approach
237 (Supplementary Figure 4) to determine whether a given donor population has colonized
238 a given recipient based on the detection of donor subpopulations in the transplant sample,
239 in the recipient pre-FMT, and in the recipient post-FMT (see Materials and Methods,

240 Supplementary Table 5). To determine colonization outcomes, we analyzed 640
241 genome/recipient pairs for Donor A (128 donor genomes in 5 recipients) and identified 99
242 successful colonization events, 38 failed colonization events, and 503 ambiguous
243 colonization events (Supplementary Table 6). For Donor B, we analyzed 915
244 genome/recipient pairs (183 donor genomes in 5 recipients) and identified 106 successful
245 colonization events, 109 failed colonization events, and 700 ambiguous colonization
246 events (Supplementary Table 6). Our stringent criteria (see Materials and Methods,
247 Supplementary Figure 4) classified the vast majority of all genome/recipient pairs as
248 ambiguous colonization events. Nevertheless, due to the relatively large number of donor
249 MAGs and FMT recipients in our study, we were left with 352 MAG/recipient pairs with
250 unambiguous phenotypes for downstream analyses.

251 Adaptive ecological forces are the primary drivers of microbial 252 colonization

253 The ability of a microbial population to colonize and persist in a complex ecosystem is
254 influenced by both neutral and adaptive forces (Maignien et al. 2014). Although which of
255 these is the major driver of successful colonization of the human gut remains unclear
256 (Smillie et al. 2018). In the context of FMT, previous studies have suggested neutral
257 processes to determine colonization success based on the abundance of a microbial
258 population in a donor stool sample (Smillie et al. 2018; Podlesny and Florian Fricke 2020).
259 Indeed, ecological drift may have a significant role in a system dominated by neutral
260 processes, where low-abundance donor populations in the transplant would be less likely
261 to be observed in recipients. In contrast, if the system is dominated by adaptive forces,
262 colonization success would be a function of the population fitness in the recipient
263 environment, rather than its abundance in the transplant.

264 To investigate the impact of neutral versus adaptive processes on colonization in our
265 dataset we first asked whether the prevalence of a donor population in healthy human gut
266 metagenomes, which we define here as a measure of its fitness, was associated with the
267 detection of the same population in donor or recipient metagenomes. Within both FMT
268 cohorts, the mean detection of each population in recipients post-FMT had a stronger

269 association with population fitness than mean detection in donor samples (Figure 2a).
270 The fitness of donor A populations explained 4.2% of the variation in mean detection of
271 those populations in donor samples ($R^2=0.042$, $p=0.021$) and 19% of variation in mean
272 detection in recipient post-FMT samples ($R^2=0.19$, $p=2.7e-07$), an increase of
273 approximately 4.5-fold (Figure 2a). Similarly, Donor B population fitness explained 7.3%
274 of the variation in mean detection in donor samples ($R^2=0.073$, $p=2.1e-04$), and 36% of
275 the variation in mean detection in recipient post-FMT samples ($R^2=0.36$, $p=4.5e-19$), an
276 increase of approximately 5-fold (Figure 2a). This suggests that fitness is a better
277 predictor of colonization outcome than it is of the detection of a population in the donor,
278 suggesting that adaptive forces are likely at play. But detecting a donor population in a
279 recipient post-FMT metagenome through metagenomic read recruitment does not prove
280 colonization, since donor genomes can recruit reads from recipient populations that are
281 closely related (i.e., strain variants) and that were low abundance prior to FMT. Single-
282 nucleotide variants in read recruitment results, however, can reveal such cases (Denef
283 2019) and quantify their dynamics (Quince et al. 2017). Thus, we developed an improved
284 model that took into consideration the presence and absence of distinct subpopulations
285 in our data and their origins (Supplementary Figure 4). We then used this model to test if
286 colonization success was correlated with population fitness or population dose, which we
287 define here as the relative abundance of a given population in the transplanted donor
288 stool sample. For Donor A populations, colonization outcome was significantly correlated
289 with both dose (Wald test, $AUC=0.73$, $p=7.7e-05$) and fitness (Wald test, $AUC=0.76$,
290 $p=6.3e-06$) (Figure 2b,c). But combining both measures as predictive variables did not
291 substantially improve the performance of our colonization model ($AUC=0.82$) (Figure 2c).
292 This was likely due to the small, but significant, correlation between dose and fitness in
293 Donor A MAGs ($R^2=0.053$, $p=0.0070$) (Figure 2d). When the fitness of a microbial
294 population is reflected in its relative abundance, the effect of fitness on colonization
295 outcome may be masked by an apparent dose effect. In contrast to Donor A, the fitness
296 of Donor B populations and their relative abundance in Donor B samples were not
297 correlated ($R^2=0.0012$, $p=0.61$) (Figure 2d), providing us with an ideal case to analyze
298 these two factors independently. Indeed, there was no correlation between dose of a
299 microbial population in Donor B transplant samples and colonization outcome in

300 recipients post-FMT (Wald test, AUC=0.56, p=0.09). Instead, we found a significant
301 correlation between the fitness of each population and the colonization outcome (Wald
302 test, AUC=0.70, p=9.0e-07) (Figure 2c).

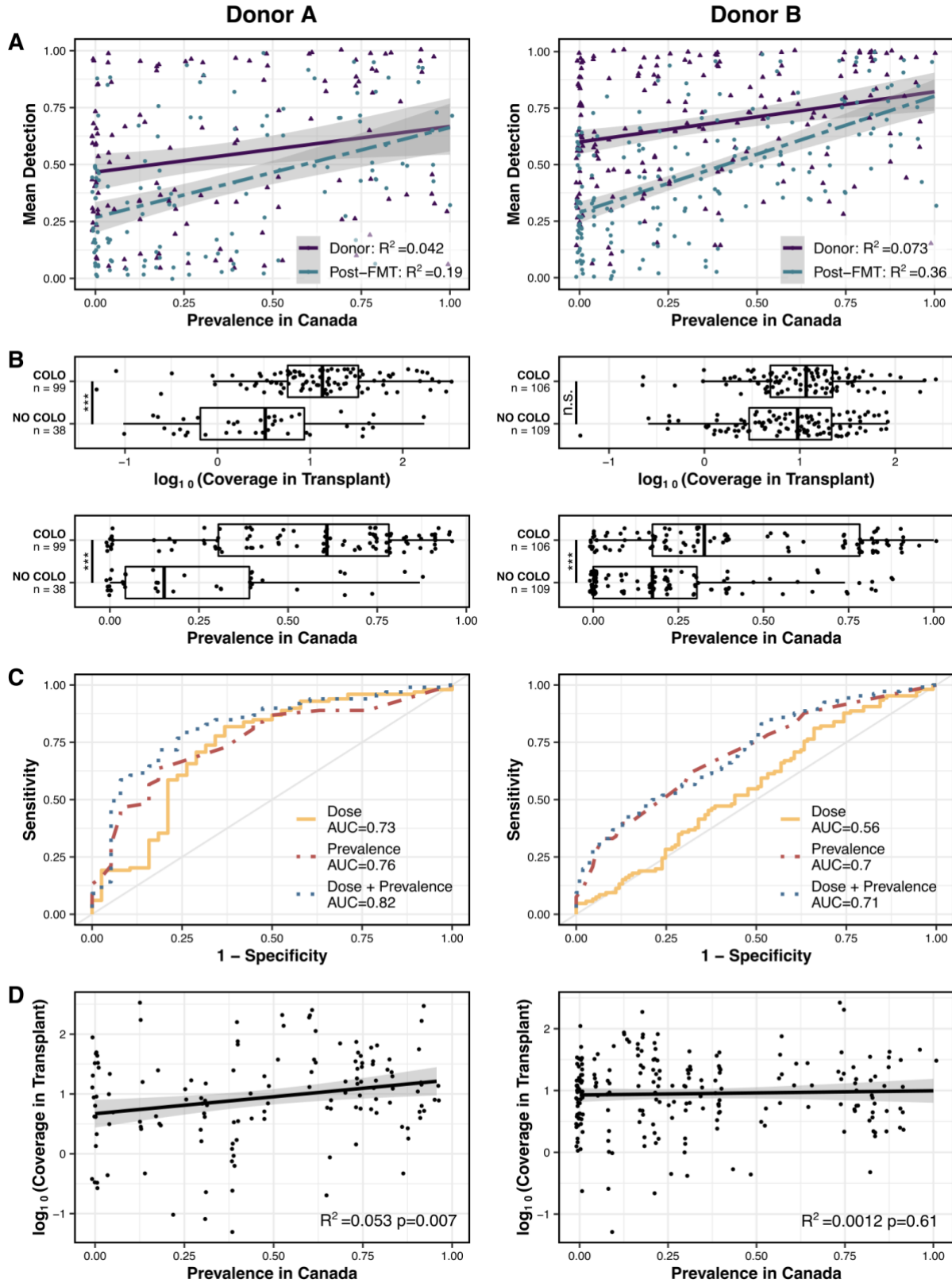
303 Taken together, our findings suggest that fitness of a microbial population as measured
304 by its prevalence across global gut metagenomes can predict its colonization success
305 better than its abundance in the donor stool sample, giving credence to the role of
306 adaptive rather than neutral ecological processes in colonization. This finding contrasts
307 with previous studies which suggested that the abundance of a given population in the
308 donor sample was an important determinant of colonization (Smillie et al. 2018; Podlesny
309 and Florian Fricke 2020). However, these analyses included many recipient samples
310 collected less than one week after FMT and it is likely that their observations were
311 influenced by the presence of transient populations. Indeed, samples collected
312 immediately after FMT are more likely to inflate the number of colonization events,
313 whereas longitudinal sampling over a longer time course can distinguish transient
314 populations from those that successfully colonized the recipients. We cannot definitively
315 test this hypothesis as we sampled most of our recipients a week after FMT. Still, on
316 average 12% of the donor populations detected in our recipients a week after FMT were
317 no longer detected after a month (Figure 1, Supplementary Table 3). Overall, our stringent
318 criteria to determine colonization outcome and the extended post-FMT sampling period
319 likely enabled us to study the long-term engraftment of successful and potentially low-
320 abundance colonizers, instead of high-abundance transient populations that may be
321 dominant directly after FMT.

322

323

324 **Figure 2. Relationships between dose, prevalence, and colonization outcome.** Left: Donor A. Right: Donor B. a)
325 Linear regression models of mean detection of each MAG in either donor or recipient post-FMT samples as a function
326 of prevalence. b) Colonization outcome of MAG/recipient pairs as a function of MAG dose or MAG prevalence.
327 Significance calculated by Wald test. c) Receiver operator curves (ROCs) for logistic regression models of colonization.
328 d) Linear regression models of dose as a function of prevalence.

329



331 Accurately distinguishing the role of dose versus fitness in colonization success is further
332 compounded by the fact that microbial populations that are prevalent across human
333 populations may also tend to be more abundant. This is well illustrated by Donor A.
334 Fortunately, the abundant populations in Donor B did not reflect prevalent microbes in
335 healthy adult guts, which demonstrated the importance of fitness as a determinant of
336 colonization success compared to dose without the confounding effect of a correlation
337 between fitness and dose. Thus, it is a theoretical possibility that colonization success is
338 purely driven by adaptive forces and is not influenced by dose, at all. However, while our
339 data assign a larger role to adaptive forces with confidence, a more accurate
340 determination of the proportional influence of adaptive versus neutral processes in
341 colonization requires a much larger dataset.

342 Colonizer and resilient microbes are enriched in metabolic 343 pathways for the biosynthesis of essential organic compounds

344 Fitness in a specific environment is conferred to an organism by a combination of
345 functional traits. In the human gut, such traits drive microbial community succession and
346 structure as a response to changing host diet and lifestyle (Koenig et al. 2011; Rothschild
347 et al. 2018). Behind successful colonization and resilience after perturbation are likely
348 similar functional traits that promote fitness. Building on our observation that suggests a
349 primary role of adaptive ecological processes in colonization outcome, we next sought to
350 identify genetic determinants of colonization. For this, we leveraged our access to donor
351 microbial population genomes and global metagenomes to investigate whether a
352 functional enrichment analysis could reveal predictors of success independent of
353 taxonomy.

354 To generate metabolic insights into colonization success we divided our donor
355 populations into 'high-fitness' and 'low-fitness' groups by considering both their
356 prevalence in FMT recipients and prevalence across global gut metagenomes (Materials
357 and Methods). The 'high-fitness' group included the microbial populations that colonized
358 or persisted in all FMT recipients and were the most prevalent in gut metagenomes from
359 Canada. We assumed that they represented a set of highly fit microbial populations as

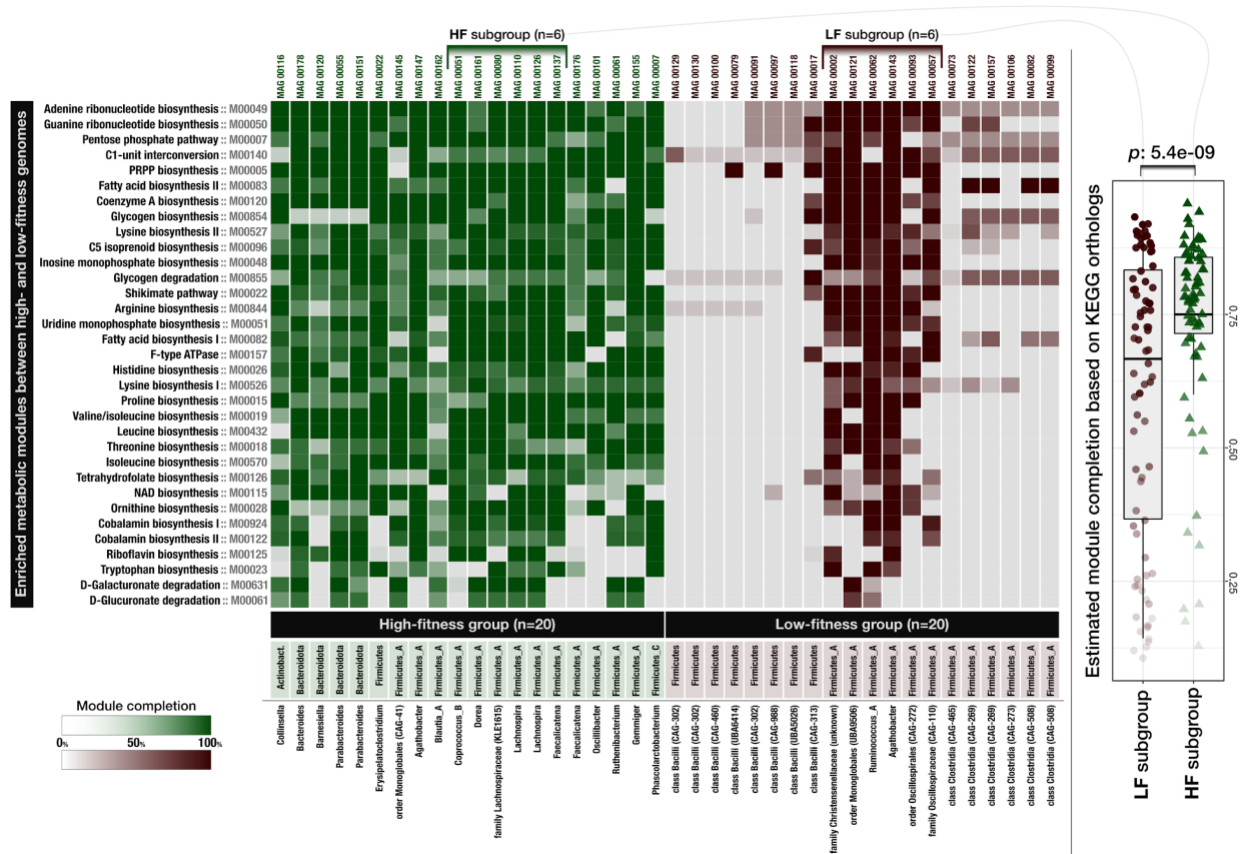
360 (1) they were able to colonize human gut environments systematically, (2) they persisted
361 in these environments long-term regardless of the host genetics or lifestyle, and (3) they
362 were prevalent in gut metagenomes outside of our study. In comparison, the ‘low-fitness’
363 group comprised microbial populations that failed to colonize or persist in at least three
364 FMT recipients. These populations were nevertheless viable gut microbes as not only our
365 long-term sampling of the donors systematically identified them but also, they sporadically
366 colonized some FMT recipients. Yet, unlike those in the high-fitness group, the distribution
367 patterns of low-fitness populations were sparse, not only within our cohort, but also within
368 publicly available metagenomes. In fact, low-fitness genomes were on average less
369 prevalent than high-fitness genomes in each of the 17 different countries we queried
370 (Supplementary Table 3). Overall, we conservatively categorized 20 populations in each
371 group for downstream analyses (Supplementary Table 7). All populations in the low-
372 fitness group resolved to Firmicutes. The high-fitness group was also dominated by
373 Firmicutes (15 of 20) but it also included five Bacteroidetes and one Actinobacteria
374 (Supplementary Table 7). Genome completion estimates did not differ between high and
375 low-fitness groups (Wilcoxon rank sum test, $p=0.42$) and averaged to 91% and 93%,
376 respectively. However, genome sizes between the two groups differed dramatically
377 ($p=2.9e-06$), where high-fitness group genomes averaged to 2.8 Mbp while low-fitness
378 group genomes averaged to 1.6 Mbp. These results suggest that the length difference
379 between genomes in high and low-fitness groups is likely to have biological relevance.
380 Indeed, we found a very high correspondence between the lengths of our MAGs and their
381 best matching reference genomes in the GTDB ($r=0.88$, $p=5e-14$) (Supplementary Table
382 7).

383 Our metabolic enrichment analysis revealed 33 KEGG pathway modules, each containing
384 genes that form a functional unit in a metabolic pathway. Every module that was enriched
385 differentially between these two groups were enriched in the high-fitness group. The lack
386 of any enriched modules in the low-fitness group is in line with the reduction in genome
387 lengths in the low-fitness group and further suggests that the reduction is associated with
388 the absence of metabolic modules. Of all enriched modules, 79% were modules related
389 to biosynthesis, which indicates an overrepresentation of biosynthetic capabilities in the
390 high-fitness group as KEGG modules for biosynthesis only make up 55% of all KEGG

391 modules (Figure 3, Supplementary Table 7). Of the 33 enriched modules, 48.5% were
392 associated with amino acid metabolism, 21.2% with vitamin and cofactor metabolism,
393 18.2% with carbohydrate metabolism, 6% with lipid metabolism and 3% with energy
394 metabolism (Supplementary Table 7). Metabolic modules that were enriched in the high-
395 fitness group included the biosynthesis of seven of the nine essential amino acids,
396 indicating the importance of metabolic competency to synthesize high-demand
397 compounds as a factor increasing fitness in colonizing new gut environments
398 (Supplementary Table 7). This is further supported by the enrichment of biosynthesis
399 pathways for the essential cofactor vitamin B12 (cobalamin), which occurred in 67.5% of
400 the high-fitness populations and only 12.5% of the low-fitness group (Supplementary
401 Table 7). Vitamin B12 is structurally highly complex and costly to produce, requiring
402 expression of more than 30 genes that are exclusively encoded by bacteria and archaea
403 (Martens et al. 2002). Thus, the competitive advantages conferred by metabolic
404 autonomy appear to outweigh the additional costs. In addition to the biosynthesis of
405 tetrahydrofolate, riboflavin, and cobalamin, the high-fitness group had a larger
406 representation of biosynthetic modules for vitamins including biotin, pantothenate, folate,
407 and thiamine (Supplementary Table 7), micronutrients that are equally important in
408 bacterial and human metabolism and are shown to play important roles in mediating host-
409 microbe interactions (Biesalski 2016). Interestingly, enriched metabolic modules in our
410 analysis partially overlap with those that Feng et al. identified as the determinants of
411 microbial fitness using metatranscriptomics and a germ-free mouse model
412 conventionalized with microbial isolates of human origin (Feng et al. 2020).

413 Even though enriched metabolic modules occurred mostly in high-fitness populations, we
414 did find some of these modules in the low-fitness group as well (Supplementary Table 7),
415 but their distribution was not uniform as they primarily occurred only in a subset of
416 genomes that resolved to Firmicutes (Figure 3). We then sought to identify whether the
417 levels of completion of these modules that occurred in both groups were identical. For
418 this, we matched six low-fitness genomes that encoded modules enriched in high-fitness
419 group genomes to six high-fitness genomes from the same phylum (marked as HF and
420 LF subgroups in Figure 3). Bacterial single-copy core genes estimated that genomes in
421 both subgroups were highly complete with a slight increase in average completion of low-

422 fitness genomes (93.7%) compared to high-fitness genomes (90.1%). Despite the higher
 423 estimated genome completion for low-fitness populations, estimated metabolic module
 424 completion values were significantly lower in the low-fitness group (Wilcoxon rank sum
 425 test with continuity correction, $V=958$, $p=5e-09$) (Figure 3, Supplementary Table 7). This
 426 indicates that even when modules that are associated with high-fitness were detected in
 427 low-fitness genomes, they were systematically missing genes and were less complete
 428 than the same modules in high-fitness genomes.



429
 430 **Figure 3.** Distribution of metabolic modules across low and high-fitness genomes. Each data point in this
 431 heat map shows the level of completion of a given metabolic module in a given genome (columns).
 432 The box-plot on the right-side compares a subset of low-fitness (LF) and high-fitness (HF) genomes, where
 433 each data point is the level of completion of a given metabolic module in a genome and shows a statistically
 434 significant difference between the overall completion of metabolic modules between these subgroups
 435 (Wilcoxon rank sum test, $p=5.4e-09$).

436 While gut microbial ecosystems of healthy individuals include both
437 low- and high-fitness microbes, IBD primarily selects for high-
438 fitness populations

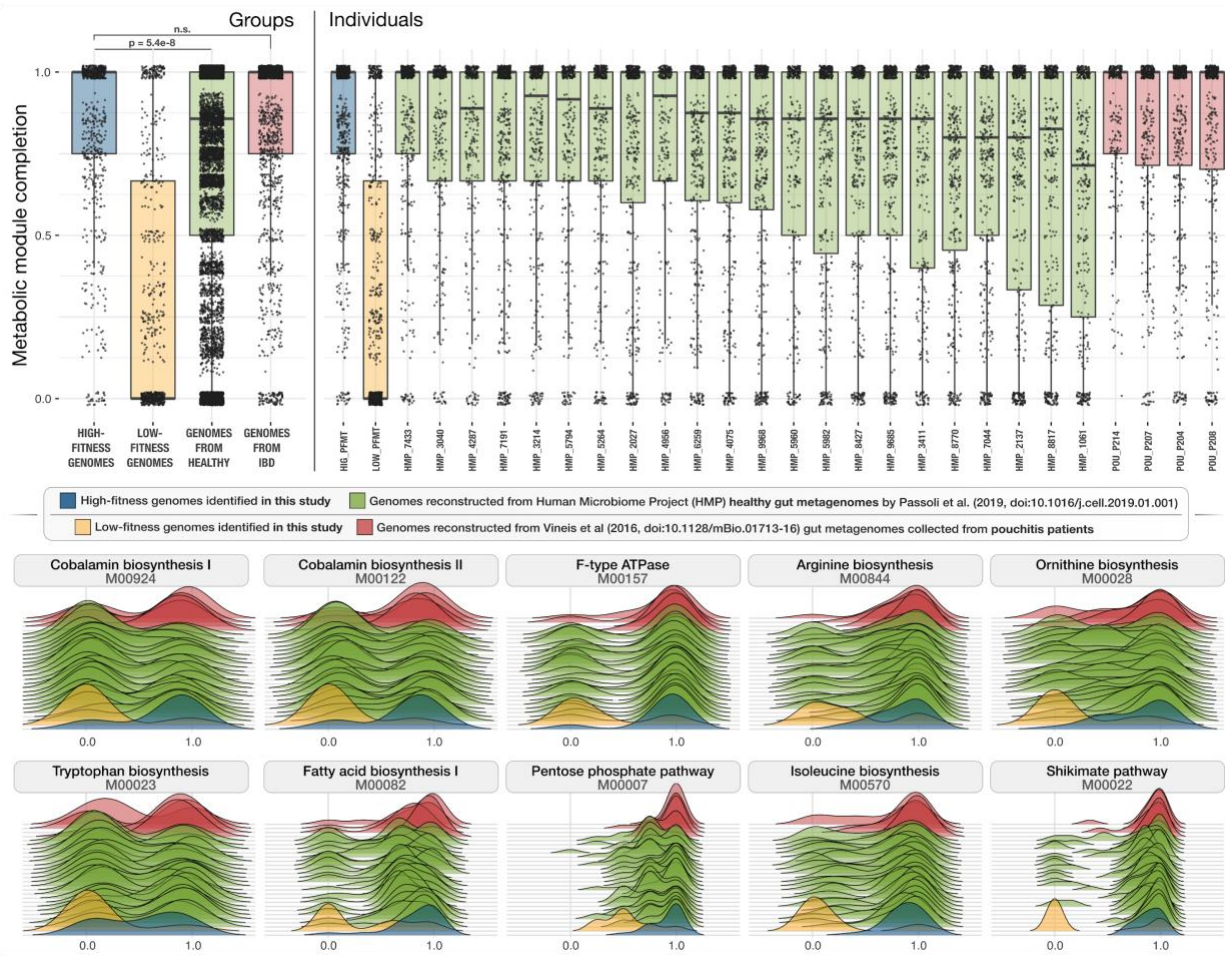
439 Our results so far show that while the healthy donor environment could support both high-
440 fitness and low-fitness populations (Figure 1, Supplementary Table 3), challenging
441 microbes to colonize a new environment or withstand massive ecosystem perturbation
442 during FMT selects for high-fitness populations (Figure 3, Supplementary Table 7),
443 suggesting that metabolic competence is a more critical determinant of fitness during
444 stress than during homeostasis. Based on these observations, it is conceivable to
445 hypothesize that (1) a healthy gut environment will support a range of microbial
446 populations with a wide spectrum of metabolic competency, and (2) a gut environment
447 under stress will select for high metabolic competency in microbial populations.

448 To test these hypotheses, we compared genomes reconstructed from a cohort of healthy
449 individuals (Pasolli et al. 2019) to genomes reconstructed from a cohort of pouchitis
450 patients (Vineis et al. 2016), a form of IBD with similar pathology to ulcerative colitis (De
451 Preter et al. 2009). We conservatively excluded genomes that were less than 70%
452 complete from the Pasolli et al. dataset to avoid underestimating pathway completion in
453 genomes from healthy people. In contrast, we included any genomes from the Vineis et
454 al. dataset if they were more than 50% complete. The number of genomes per individual
455 and their level of completeness were similar between IBD and healthy individuals: we
456 compared 44 genomes from 4 IBD patients with an average completion of 89.2% and 264
457 genomes from 22 healthy individuals with an average completion of 90.4%
458 (Supplementary Table 8). Intriguingly, similar to the length differences between genomes
459 of high-fitness and low-fitness populations (2.8 Mbp versus 1.6 Mbp on average),
460 microbial populations associated with IBD patients had larger genomes compared to
461 healthy people and averaged to 3.3 Mbp versus 2.6 Mbp, respectively (Supplementary
462 Table 8). This suggests that despite the slightly higher completion of microbial genomes
463 from the healthy cohort, these genomes tended to be smaller in size than the genomes
464 reconstructed from IBD patients.

465 Next, we asked whether the completion of those metabolic modules associated with
466 colonization success and resilience differed between the genomes reconstructed from
467 healthy and IBD individuals. The level of completion of the 33 metabolic modules were
468 almost identical between high-fitness genomes and genomes from IBD patients
469 (Wilcoxon rank sum test, $p=0.5$), but they were significantly less complete in microbial
470 genomes from healthy individuals (Wilcoxon rank sum test, $p=5.39e-08$) (Figure 4,
471 Supplementary Table 8). Metabolic modules with the largest differences in completion
472 between genomes from healthy and IBD individuals included biosynthesis of cobalamin,
473 arginine, ornithine, tryptophan, isoleucine as well as the Shikimate pathway (Figure 4,
474 Supplementary Table 8), a seven step metabolic route bacteria use for the biosynthesis
475 of aromatic amino acids (phenylalanine, tyrosine, and tryptophan) (Herrmann and Weaver
476 1999).

477 Our findings show that the same set of key metabolic modules that distinguish high-fitness
478 and low-fitness populations in FMT were also differentially associated with populations
479 that occurred in healthy individuals compared to IBD patients. In particular, while healthy
480 individuals seem to harbor microbes with a broad range of metabolic competency, IBD
481 individuals appear to be enriched with organisms with metabolic autonomy. It is
482 conceivable that a stable gut microbial ecosystem is more likely to support low-fitness
483 populations through metabolic cross-feeding, where vitamins, amino acids, and
484 nucleotides are exchanged between microbes (D'Souza et al. 2018). In contrast, host-
485 mediated environmental stress in IBD likely disrupts such interactions and creates an
486 ecological filter that selects for metabolic competence, which subsequently leads to loss
487 of diversity and the dominance of organisms with large genomes that are not necessarily
488 abundant in states of homeostasis.

489 **Figure 4.** Distribution of metabolic modules in genomes reconstructed from healthy individuals and
490 individuals with IBD. The top panel shows the metabolic module completion values for (1) high- and (2) low-
491 fitness donor genomes identified in this study (blue and orange), (3) genomes from healthy individuals
492 (green), and (4) genomes from individuals with IBD. Next to group averages, shown the distribution of
493 metabolic modules for each individual. Each dot in a given box-plot represents one of 33 metabolic modules
494 that were enriched in high-fitness FMT donor populations and the y-axis indicates its estimated completion.
495 In the bottom panel the completion values for 10 of the 33 pathways shown as ridge-line plots.



496

497 These observations have implications for the defining features of healthy gut
498 environments from an ecological point of view. Defining the 'healthy gut microbiome' has
499 been a major goal of human gut microbiome research (Bäckhed et al. 2012), and remains
500 elusive (Eisenstein 2020). Despite comprehensive investigations that considered core
501 microbial taxa (Arumugam et al. 2011; Lloyd-Price, Abu-Ali, and Huttenhower 2016) or
502 guilds of microbes that represent coherent functional groups (Wu et al. 2021), the search
503 for 'biomarkers' of healthy microbiomes is ongoing (McBurney et al. 2019). Given our data
504 we hypothesize that one of the defining features of a healthy gut environment is its ability
505 to support a diverse community of microbes with a broad spectrum of metabolic
506 competence, where both low-fitness and high-fitness populations live in a coherent
507 ecosystem. Conversely, an enrichment of metabolically competent high-fitness
508 populations would likely indicate the presence of environmental stress. Our analyses
509 demonstrate that this is a quantifiable feature of microbial communities through genome-

510 resolved metagenomic surveys, although testing this hypothesis rigorously requires a
511 larger number of genomes reconstructed from a larger number of individuals diagnosed
512 with a broader set of IBDs. Our analyses have other limitations. For instance, metabolic
513 insights in our study have been limited to genomic potential and have considered only
514 well-known metabolic pathways, which, given the extent of the unknown coding space in
515 microbial genomes (Vanni et al. 2020), are likely far from complete. As a result, the
516 disproportional enrichment of biosynthetic modules in high-fitness genomes indicates that
517 the ability to synthesize essential biological compounds is necessary but likely insufficient
518 to survive environmental stress in the gut. Nevertheless, the finding that the same
519 metabolic modules that promote colonization success after FMT are also the hallmarks
520 of fitness in IBD suggests the presence of ecological principles that are shared between
521 these systems and warrants deeper investigation.

522 Subtle differences in key functions distinguish populations of the 523 same genus with differential colonization success

524 While adaptive processes that favor metabolic independence explain the determinants of
525 colonization and resilience for distantly related taxa, metabolic features that promote high-
526 fitness at this broad level may not explain differences in fitness between more closely
527 related taxa, such as distinct species within a single genus, which are likely to have similar
528 metabolic capabilities (Martiny, Treseder, and Pusch 2013) due to unifying ecological
529 traits in higher ranks of taxonomy (Philippot et al. 2010). We finally investigated whether
530 we could identify determinants of fitness across metabolically similar populations with
531 different levels of success in colonizing unrelated individuals.

532 Members of the genus *Bifidobacterium* have long been used as probiotics (Gomes and
533 Malcata 1999) and are prevalent occupants of the healthy human gut microbiota
534 (Arboleya et al. 2016). In our dataset, *Bifidobacterium* was the second most abundant
535 genus (14.1%) after *Bacteroides* (15.8%) in Donor A, from whom we reconstructed three
536 MAGs over 98% completion that resolved to three distinct species in this genus: *B.*
537 *longum*, *B. adolescentis* subsp. *adolescentis*, and *B. animalis* subsp. *lactis*
538 (Supplementary Table 3). While each of these *Bifidobacterium* populations occurred in

539 Donor A metagenomes in a relatively stable fashion, they showed vastly different
540 colonization efficiency upon FMT (Figure 5), enabling us to investigate determinants of
541 colonization among closely related taxa.

542 In contrast to the *B. longum* and *B. adolescentis* subsp. *adolescentis* (henceforth *B.*
543 *adolescentis*) populations that colonized most recipients, *B. animalis* subsp. *lactis*
544 (henceforth *B. lactis*) did not seem to have colonized any of our recipients (Supplementary
545 Table 3). Overall, we were able to detect *B. longum*, *B. adolescentis*, and *B. lactis*
546 populations in 83%, 75%, and 4% of all post-FMT recipient metagenomes, respectively
547 (Figure 5). Most strikingly, patterns of colonization that emerged from the analysis of FMT
548 recipients reflected those seen in publicly available gut metagenomes from Canada,
549 where *B. longum*, *B. adolescentis*, and *B. lactis* populations occurred in 74%, 39%, and
550 13% of the population, demonstrating a positive relationship (Pearson's correlation of 0.9,
551 n.s.) between the colonization efficiency upon FMT and the fitness of these populations.
552 Furthermore, the gut metagenomes from 17 countries confirmed the substantially
553 reduced fitness of *B. lactis* globally (Supplementary Table 9). Interestingly, the *B. lactis*
554 MAG we reconstructed from Donor A was virtually identical (with over 99.99% sequence
555 identity over 99.82% alignment, Supplementary Table 9) to most *B. lactis* strains that are
556 widely used as probiotics (Jungersen et al. 2014), revealing a disagreement between the
557 preferences of commercial microbial therapeutics and human gut microbial ecology.

558

559

560 **Figure 5. Characteristics of three *Bifidobacterium* species.** Top panel shows the distribution of Donor A MAGs that
561 represent three distinct *Bifidobacterium* populations across donor and recipient metagenomes before and after FMT.
562 The last two columns in this panel show the prevalence of these populations in post-FMT metagenomes, and publicly
563 available gut metagenomes from Canada. The panel below displays the distribution of KEGG orthologs across the
564 three *Bifidobacterium* MAGs along with 31 high-quality isolate genomes from the NCBI. Each item shown in concentric
565 circles represents a single function assigned by the database of KEGG Orthologs, and each layer is a distinct genome.
566 The intensity of color indicates the presence of a given function in a given genome. The most outer circle marks groups
567 of functions that are enriched in various groups of *Bifidobacterium* genomes as well as those functions that are not
568 enriched in any group as they are either in all genomes, or only a very small number of them.

582 qualifies this group as attractive probiotics (Strozzi and Mogna 2008; Pompei et al. 2007),
583 but this pathway was absent in *B. lactis* genomes. We also found that *B. longum* and *B.*
584 *adolescentis* genomes encoded histidine and nicotinamide adenine dinucleotide (NAD)
585 biosynthesis which *B. lactis* lacked (Supplementary Table 9). Finally, the average genome
586 lengths of *B. longum* (2.31 Mbp) and *B. adolescentis* (2.18 Mbp) were longer than the
587 average genome length of *B. lactis* (1.94 Mbp), which reflects the pattern we observed
588 previously where high-fitness populations tended to have larger genomes. In summary,
589 even though all *Bifidobacterium* genomes in our pangenome had a higher metabolic
590 overlap with one another compared to high-fitness and low-fitness genomes we have
591 previously studied, the reduced fitness of *B. lactis* compared to *B. longum* and *B.*
592 *adolescentis* could still be explained by the absence of a small number of metabolic
593 competencies associated with the high-fitness group genomes.

594 Next, we focused on the enrichment of individual functions across the three groups of
595 genomes using gene annotations from KOfam profiles (Aramaki et al. 2020) from the
596 Kyoto Encyclopedia of Genes and Genomes (KEGG) (M. Kanehisa and Goto 2000) and
597 Clusters of Orthologous Groups (COGs) from the NCBI (Galperin et al. 2021). Of all 954
598 unique KOfams found in our *Bifidobacterium* pangenome, 272 functions were not
599 common to all genomes but statistically enriched in either one or two groups. Our analysis
600 of these accessory functions showed that *B. longum* encoded 150 (55.5%), *B.*
601 *adolescentis* encoded 115 (42.3%), and *B. lactis* encoded 95 (34.9%) of all accessory
602 functions that were statistically enriched (Figure 5, Supplementary Table 9). The same
603 analysis with 1,286 unique COGs confirmed these observations: of all 353 COGs
604 enriched in any group, *B. longum* encoded 212 (60.1%), *B. adolescentis* encoded 172
605 (48.7%), and *B. lactis* encoded 118 (33.4%) (Supplementary Table 9). Overall, these
606 results reveal a striking correlation between the number of accessory functions
607 associated with *B. longum*, *B. adolescentis*, and *B. lactis*, and echo the absence of
608 metabolic pathways in *B. lactis* even at the level of accessory gene functions, explaining
609 their differential ability to colonize new individuals and distribution in global human gut
610 metagenomes.

611 We finally investigated the contents of the differentially occurring accessory functions to
612 speculate on whether they could be related to differences in fitness. For instance, in
613 contrast to all *B. longum* and *B. adolescentis* in the *Bifidobacterium* pangenome, none of
614 the *B. lactis* genomes encoded a phosphoenolpyruvate phosphotransferase (PEP-PTS)
615 system specific for the uptake of β -glucoside (Supplementary Table 9). As the genus
616 *Bifidobacterium* is characterized by a large array of genes associated with carbohydrate
617 uptake and metabolism (Ventura et al. 2009; Schell et al. 2002; Kleerebezem and
618 Vaughan 2009), *B. lactis* represents a notable exception with a lower number of genes
619 associated with carbohydrate metabolism, fewer genes encoding carbohydrate-specific
620 ABC transporters, and the absence of phosphoenolpyruvate-phosphotransferase (PEP-
621 PTS) systems (Barrangou et al. 2009). The absence of any other PEP-PTS system in *B.*
622 *longum* and *B. adolescentis* may indicate the catabolic niche occupied by these
623 populations in the human gut that is shaped by their extensive capacity for uptake and
624 metabolism of plant derived glycosides (Chien, Huang, and Chou 2006; Schell et al.
625 2002). Additional functions that exclusively occurred in *B. adolescentis* and *B. longum*
626 genomes included two multidrug resistance pumps of the ‘multidrug and toxin extrusion’
627 (MATE) type, three transporters of the major facilitator superfamily (MFS) involved in bile
628 acid tolerance and macrolide efflux, two bile acid:sodium ion symporters, and one
629 proton/chloride ion antiporter conferring acid tolerance (Supplementary Table 9). The
630 drug defense mechanisms may act to protect these populations during periods of
631 inflammation and drug administration, but may also be beneficial with regard to the
632 common ingestion of antibiotics through various food products (Kirchhelle 2018). These
633 results show that in the microbial fitness landscape of the human gut, where the
634 determinants of success across distantly related taxa are primarily defined by the
635 presence or absence of a large number of metabolic pathways, there exists smaller
636 niches equally accessible to closely related organisms with similar metabolic potential,
637 among which success can be speculated by subtle differences in key functions.

638 Conclusions

639 Our study points to adaptive ecological processes as primary determinants of both long-
640 term colonization after FMT and microbial fitness in the human gut environment through
641 metabolic competency as conferred by biosynthesis of nucleotides, amino acids, and
642 essential micronutrients. Even when we found these metabolic modules in low-fitness
643 populations, they were systematically less complete compared to their high-fitness
644 counterparts.

645 Our findings suggest that in a healthy gut environment high- and low-fitness populations
646 co-occur in harmony, with their differential fitness indiscernible by taxonomy or relative
647 abundance. However, transfer to a new gut environment through FMT, or host-mediated
648 stress through IBD, initiates an ecological filter that selects for high-fitness populations
649 that can self-sustain. This model offers a null hypothesis to explain how low-abundance
650 members of healthy gut environments can come to dominate the gut microbiota under
651 stressful conditions, while not being causally associated with disease states. If the
652 association between particular microbial taxa and disease is solely driven by their
653 superior metabolic competence, microbial therapies that aim to treat complex diseases
654 by adding microbes associated with healthy individuals will be unlikely to compete with
655 the adaptive processes that regulate complex gut microbial ecosystems.

656

657 Materials and Methods

658 **Sample collection and storage.** We used a subset of individuals who participated in a
659 randomized clinical trial (Kao et al. 2017) and conducted a longitudinal FMT study of two
660 human cohorts (DA and DB), each consisting of one FMT donor and 5 FMT recipients of
661 that donor's stool. All recipients received vancomycin for a minimum of 10 days pre-FMT
662 at a dose of 125 mg four times daily. Three DA and two DB recipients received FMT via
663 pill, and two DA and three DB recipients received FMT via colonoscopy. All recipients had
664 recurrent *C. difficile* infection before FMT, and two DA recipients and 1 DB recipient were
665 also diagnosed with ulcerative colitis (UC). 24 stool samples were collected from the DA
666 donor over a period of 636 days, and 15 stool samples were collected from the DB donor
667 over a period of 532 days. Between 5 and 9 stool samples were collected from each
668 recipient over periods of 187 to 404 days, with at least one sample collected pre-FMT and
669 2 samples collected post-FMT. This gave us a total of 109 stool samples from all donors
670 and recipients. Samples were stored at -80°C. (Supplementary Figure 1, Supplementary
671 Table 1)

672 **Metagenomic short-read sequencing.** We extracted the genomic DNA from frozen
673 samples according to the centrifugation protocol outlined in MoBio PowerSoil kit with the
674 following modifications: cell lysis was performed using a GenoGrinder to physically lyse
675 the samples in the MoBio Bead Plates and Solution (5–10 min). After final precipitation,
676 the DNA samples were resuspended in TE buffer and stored at -20 °C until further
677 analysis. Sample DNA concentrations were determined by PicoGreen assay. DNA was
678 sheared to ~400 bp using the Covaris S2 acoustic platform and libraries were constructed
679 using the Nugen Ovation Ultralow kit. The products were visualized on an Agilent
680 Tapestation 4200 and size-selected using BluePippin (Sage Biosciences). The final
681 library pool was quantified with the Kapa Biosystems qPCR protocol and sequenced on
682 the Illumina NextSeq500 in a 2 × 150 paired-end sequencing run using dedicated read
683 indexing.

684 **'Omics workflows.** Whenever applicable, we automated and scaled our 'omics analyses
685 using the bioinformatics workflows implemented by the program `anvi-run-workflow`

686 (Shaiber et al. 2020) in anvi'o (Eren et al. 2015, 2021). Anvi'o workflows implement
687 numerous steps of bioinformatics tasks including short-read quality filtering, assembly,
688 gene calling, functional annotation, hidden Markov model search, metagenomic read-
689 recruitment, metagenomic binning, pangenomics, and phylogenomics. Workflows use
690 Snakemake (Köster and Rahmann 2012) and a tutorial is available at the URL
691 <http://merenlab.org/anvio-workflows/>. The following sections detail these steps.

692 **Taxonomic composition of metagenomes based on short reads.** We used Kraken2
693 v2.0.8-beta (Wood, Lu, and Langmead 2019) with the NCBI's RefSeq bacterial, archaeal,
694 viral and viral neighbours genome databases to calculate the taxonomic composition
695 within short-read metagenomes.

696 **Assembly of metagenomic short and long reads.** To minimize the impact of random
697 sequencing errors in our downstream analyses, we used the program `iu-filter-quality-
698 minoche` to process short metagenomic reads, which is implemented in illumina-utils
699 v2.11 (Eren et al. 2013) and removes low-quality reads according to the criteria outlined
700 by Minoche et al. (Minoche, Dohm, and Himmelbauer 2011). IDBA_UD v1.1.2 (Peng et
701 al. 2012) assembled quality-filtered short reads into longer contiguous sequences
702 (contigs), although we needed to recompile IDBA_UD with a modified header file so it
703 could process 150bp paired-end reads. For the assembly of long-reads and identification
704 of circular contigs we used Flye v2.6 (Kolmogorov et al. 2019) with the `--meta` argument
705 followed by Pilon v1.23 (Walker et al. 2014) correction using the high-quality short-reads.

706 **Processing of contigs.** We use the following strategies to process both sequences we
707 obtained from our assemblies and those we obtained from reference genomes. Briefly,
708 we used (1) `anvi-gen-contigs-database` on contigs to compute k-mer frequencies and
709 identify open reading frames (ORFs) using Prodigal v2.6.3 (Hyatt et al. 2010), (2) `anvi-
710 run-hmms` to identify sets of bacterial (Campbell et al. 2013) and archaeal (Rinke et al.
711 2013) single-copy core genes using HMMER v3.2.1 (Eddy 2011), (3) `anvi-run-ncbi-cogs`
712 to annotate ORFs with functions from the NCBI's Clusters of Orthologous Groups (COGs)
713 (Tatusov et al. 2003), and (4) `anvi-run-kegg-kofams` to annotate ORFs with functions
714 from the KOfam HMM database of KEGG orthologs (KOs) (Aramaki et al. 2020; M.
715 Kanehisa and Goto 2000). To predict the approximate number of genomes in

716 metagenomic assemblies we used the program `anvi-display-contigs-stats`, which
717 calculates the mode of the frequency of single-copy core genes as described previously
718 (Delmont and Eren 2016).

719 **Metagenomic read recruitment, reconstructing genomes from metagenomes,**
720 **determination of genome taxonomy and ANI.** We recruited metagenomic short reads
721 to contigs using Bowtie2 v2.3.5 (Langmead and Salzberg 2012) and converted resulting
722 SAM files to BAM files using samtools v1.9 (Li et al. 2009). We profiled the resulting BAM
723 files using the program `anvi-profile` with the flag `--min-contig-length` set to 2500 to
724 eliminate shorter sequences to minimize noise. Once we have read recruitment results
725 from each metagenome is profiled to store contig coverages into single anvi'o profile
726 databases, `anvi-merge` combined all profiles into an anvi'o merged profile for
727 downstream visualization, binning, and statistical analyses. We then used `anvi-cluster-
728 contigs` to group contigs into 100 initial bins using CONCOCT v1.1.0 (Alneberg et al.
729 2014), `anvi-refine` to manually curate initial bins with conflation error based on
730 tetranucleotide frequency and differential coverage signal across all samples, and `anvi-
731 summarize` to report final summary statistics for each gene, contig, and bin. We used the
732 program `anvi-rename-bins` to identify bins that were more than 70% complete and less
733 than 10% redundant, and store them in a new collection as metagenome-assembled
734 genomes (MAG), discarding lower quality bins from downstream analyses. GTBD-tk
735 v0.3.2 (Chaumeil et al. 2019) assigned taxonomy to each of our MAG using GTDB r89
736 (Parks et al. 2018), but to assign species- and subspecies-level taxonomy for
737 `DA_MAG_00057`, `DA_MAG_00011`, `DA_MAG_00052` and `DA_MAG_00018`, we
738 used `anvi-get-sequences-for-hmm-hits` to recover DNA sequences for bacterial single-
739 copy core genes that encode ribosomal proteins, and searched them in the NCBI's
740 nucleotide collection (nt) database using BLAST (Altschul et al. 1990). Finally, the
741 program `anvi-compute-genome-similarity` calculated pairwise genomic average
742 nucleotide identity (gANI) of our genomes using PyANI v0.2.9 (Pritchard et al. 2016).

743 **Criteria for MAG detection in metagenomes.** Using mean coverage to assess the
744 occurrence of populations in a given sample based on metagenomic read recruitment can
745 yield misleading insights since this strategy cannot accurately distinguish reference

746 sequences that represent very low-abundance environmental populations from those
747 sequences that do not represent an environmental population in a sample yet still recruit
748 reads from non-target populations due to the presence of conserved genomic regions.
749 Thus we relied upon the ‘detection’ metric, which is a measure of the proportion of the
750 nucleotides in a given sequence that are covered by at least one short read, and
751 considered a population was detected in a metagenome if `anvi'o` reported a detection
752 value of at least 0.25 for its genome (whether it was a metagenome-assembled or isolate
753 genome). Values of detection in metagenomic read recruitment results often follow a
754 bimodal distribution for populations that are present and absent (see Supplementary
755 Figure 2 in (Utter et al. 2020)), thus 0.25 is an appropriate cutoff to eliminate false-positive
756 signal in read recruitment results for populations that are absent.

757 **Identification of MAGs that represent multiple subpopulations.** To identify
758 subpopulations of MAGs in metagenomes, we used the `anvi'o` command ``anvi-gen-`
759 `variability-profile`` with the ``--quince-mode`` flag which exported single-nucleotide variant
760 (SNV) information for all MAGs after read recruitment. We then used DESMAN v2.1.1
761 (Quince et al. 2017) to analyze SNVs to determine the number and distribution of
762 subpopulations represented by a single genome. To account for non-specific mapping
763 that can inflate the number of estimated subpopulations, we removed any subpopulation
764 that made up less than 1% of the entire population explained by a single MAG. To account
765 for noise due to low-coverage, we only investigated subpopulation for MAGs for which
766 the mean non-outlier coverage of single-copy core genes was at least 10X.

767 **Criteria for colonization of a recipient by a MAG.** We developed a method to determine
768 whether or not a MAG successfully colonized a recipient, and applied this method to each
769 MAG and each recipient within a cohort. In order to confidently assign colonization or
770 non-colonization phenotypes to each MAG/recipient pair, we required that the MAG be
771 detected in the donor sample used for transplant into the recipient. If these criteria were
772 met, we then determined whether the MAG was detected in any post-FMT recipient
773 sample taken more than 7 days after transplant. If not, the MAG/recipient pair was
774 considered a non-colonization event. If the MAG was detected in the recipient greater
775 than 7 days post-FMT, we used subpopulation information to determine if any

776 subpopulation present in the donor and absent in the recipient pre-FMT was detected in
777 the recipient more than 7 days post-FMT. If this was the case, we considered this to
778 represent a colonization event. See Supplementary Figure 4 for a complete outline of all
779 possible cases.

780 **Determination of dose and fitness for MAGs.** We defined population dose as the
781 second and third quartile mean coverage of a population in the transplanted stool sample.
782 We defined fitness as the prevalence of a population in 23 healthy adult gut metagenomes
783 (see Materials and Methods: Criteria for MAG detection in metagenomes) from Canada,
784 the same country in which the FMTs were performed.

785 **Regression analysis.** To examine the association between dose and/or prevalence with
786 colonization outcome, we built binomial logistic regression models using the R stats ``glm``
787 function. We used the R stats ``predict`` function and the R pROC ``roc`` function to evaluate
788 our models by creating receiver operating characteristic (ROC) curves and calculating the
789 area under the ROC curve (AUC). To determine the correlation between dose and
790 prevalence, we performed linear regression using the R stats ``lm`` function. We used the
791 R tidyverse package, including ggplot2, to visualize boxplots, scatterplots, and ROC
792 curves.

793 **Pangenomic analysis and gANI.** We used `anvi'o` to compute and visualize pangenomes
794 of MAGs and reference genomes. We stored all processed MAG and reference genome
795 contigs (see Contig processing methods section) in an `anvi'o` database using the
796 command ``anvi-gen-genomes-storage``. To create the pangenomes, we then passed that
797 database to the command ``anvi-pan-genome`` which used NCBI's BLAST (Altschul et al.
798 1990) to quantify gene similarity within and between genomes and the Markov Cluster
799 algorithm (MCL) (Enright, Van Dongen, and Ouzounis 2002) to cluster groups of similar
800 genes. We set the ``anvi-pan-genome`` ``--min-occurrence`` flag to 2 to remove gene
801 clusters only present in one genome (singletons), and visualized pangenomes using
802 ``anvi-display-pan``.

803 **Phylogenomic tree construction.** To concatenate and align amino acid sequences of
804 46 single-copy core (Campbell et al. 2013) ribosomal proteins that were present in all of

805 our *Bifidobacterium* MAGs and reference genomes, we ran the `anvi'o` command ``anvi-`
806 `get-sequences-for-hmm-hits`` with the ``--return-best-hit``, ``--get-aa-sequence`` and ``--`
807 `concatenate`` flags, and the ``--align-with`` flag set to ``muscle`` to use MUSCLE v3.8.1551
808 (Edgar 2004) for alignment. We then ran ``anvi-gen-phylogenomic-tree`` with default
809 parameters to compute a phylogenomic tree using FastTree 2.1 (Price, Dehal, and Arkin
810 2010).

811 **Analysis of metabolic modules and enrichment.** We calculated the level of
812 completeness for a given KEGG module (Minoru Kanehisa et al. 2014, 2017) in our
813 genomes using the program ``anvi-estimate-metabolism``, which leveraged previous
814 annotation of genes with KEGG orthologs (KOs) (see the section 'Processing of contigs').
815 Then, the program ``anvi-compute-functional-enrichment`` determined whether a given
816 metabolic module was enriched in based on the output from ``anvi-estimate-metabolism``.
817 The URL <https://merenlab.org/m/anvi-estimate-metabolism> serves a tutorial for this
818 program which details the modes of usage and output file formats. The statistical
819 approach for enrichment analysis is defined elsewhere (Shaiber et al. 2020), but briefly it
820 computes enrichment scores for functions (or metabolic modules) within groups by fitting
821 a binomial generalized linear model (GLM) to the occurrence of each function or complete
822 metabolic module in each group, and then computing a Rao test statistic, uncorrected p-
823 values, and corrected q-values. We considered any function or metabolic module with a
824 q-value less than 0.05 to be 'enriched' in its associated group if it was also at least 75%
825 complete and in at least 50% of the group members. To display the distribution of
826 individual KEGG orthologs across genomes and order them based on their enrichment
827 scores and group affiliations we used the program ``anvi-display-functions``.

828 **Determination of high-fitness and low-fitness MAGs for metabolic enrichment**
829 **analysis.** We classified MAGs as high-fitness if, in all 5 recipients, they were detected in
830 the donor sample used for transplantation as well as the recipient more than 7 days post-
831 FMT. We classified low-fitness MAGs as those that, in at least 3 recipients, were detected
832 in the donor sample used for FMT but were not detected in the recipient at least 7 days
833 post-FMT. We reduced the number of high-fitness MAGs to be the same as the number

834 of low-fitness MAGs for metabolic enrichment analysis by selecting only the high-fitness
835 MAGs which were the most prevalent in the Canadian gut metagenomes.

836 **Ordination plots.** We used the R `vegan` v2.4-2 package `metaMDS` function to perform
837 nonmetric multidimensional scaling (NMDS) with Horn-Morisita dissimilarity distance to
838 compare taxonomic composition between donor, recipient, and global metagenomes. We
839 visualized ordination plots using R `ggplot2`.

840 Data Availability

841 Raw sequencing data for donor and recipient metagenomes are stored under the NCBI
842 BioProject PRJNA701961 (see Supplementary Table 1 for accession numbers).
843 Supplementary tables are accessible via doi: [10.6084/m9.figshare.14138405](https://doi.org/10.6084/m9.figshare.14138405).

844 Acknowledgements

845 We thank Mitchell L. Sogin, Eugene B. Chang, and Howard Shuman for helpful
846 discussions, Ryan Moore (0000-0003-3337-8184) and Ozcan C. Esen (0000-0001-7337-
847 671X) for technical help. We also thank Kaiyu Wu, Robyn Louie and Linda Ward of the
848 IPC Research Laboratory at the University of Calgary for their help with patient
849 recruitment and sampling. This project was supported by the GI Research Foundation
850 (GIRF) and the Mutchnik Family Fund.

851 Author Contributions

852 AME, TL, BJ conceived the study. JZD, MS, TL recruited patients, performed
853 transplantation experiments, and collected samples. ARW, JF, AME performed primary
854 data analyses. IV developed research tools. KL, STML, HGM performed sample
855 processing and sequencing. FT, AS, EF, CQ, MKY, AY contributed to data analyses and
856 interpretation. DTR, BJ, TL, and AME directed research. ARW, JF, AME wrote the paper
857 with critical input from all authors.

858 Competing Interests

859 Authors declare no competing financial interests.

860 References

- 861 Almeida, Cátia, Rita Oliveira, Raquel Soares, and Pedro Barata. 2020. "Influence of Gut
862 Microbiota Dysbiosis on Brain Function: A Systematic Review." *Porto Biomedical*
863 *Journal* 5 (2). <https://doi.org/10.1097/j.pbj.0000000000000059>.
- 864 Alneberg, Johannes, Brynjar Smári Bjarnason, Ino de Bruijn, Melanie Schirmer, Joshua
865 Quick, Umer Z. Ijaz, Leo Lahti, Nicholas J. Loman, Anders F. Andersson, and
866 Christopher Quince. 2014. "Binning Metagenomic Contigs by Coverage and
867 Composition." *Nature Methods* 11 (11): 1144–46.
- 868 Altschul, S. F., W. Gish, W. Miller, E. W. Myers, and D. J. Lipman. 1990. "Basic Local
869 Alignment Search Tool." *Journal of Molecular Biology* 215 (3): 403–10.
- 870 Aramaki, Takuya, Romain Blanc-Mathieu, Hisashi Endo, Koichi Ohkubo, Minoru
871 Kanehisa, Susumu Goto, and Hiroyuki Ogata. 2020. "KofamKOALA: KEGG
872 Ortholog Assignment Based on Profile HMM and Adaptive Score Threshold."
873 *Bioinformatics* 36 (7): 2251–52.
- 874 Arboleya, Silvia, Claire Watkins, Catherine Stanton, and R. Paul Ross. 2016. "Gut
875 Bifidobacteria Populations in Human Health and Aging." *Frontiers in Microbiology* 7
876 (August): 1204.
- 877 Arumugam, Manimozhiyan, Jeroen Raes, Eric Pelletier, Denis Le Paslier, Takuji
878 Yamada, Daniel R. Mende, Gabriel R. Fernandes, et al. 2011. "Enterotypes of the
879 Human Gut Microbiome." *Nature* 473 (7346): 174–80.
- 880 Bäckhed, Fredrik, Claire M. Fraser, Yehuda Ringel, Mary Ellen Sanders, R. Balfour
881 Sartor, Philip M. Sherman, James Versalovic, Vincent Young, and B. Brett Finlay.
882 2012. "Defining a Healthy Human Gut Microbiome: Current Concepts, Future
883 Directions, and Clinical Applications." *Cell Host & Microbe* 12 (5): 611–22.
- 884 Barrangou, Rodolphe, Elizabeth P. Briczinski, Lindsay L. Traeger, Joseph R. Loquasto,
885 Melissa Richards, Philippe Horvath, Anne-Claire Coûté-Monvoisin, et al. 2009.
886 "Comparison of the Complete Genome Sequences of *Bifidobacterium Animalis*
887 Subsp. *Lactis* DSM 10140 and BI-04." *Journal of Bacteriology* 191 (13): 4144–51.
- 888 Baumgart, Daniel C., and Simon R. Carding. 2007. "Inflammatory Bowel Disease:
889 Cause and Immunobiology." *The Lancet* 369 (9573): 1627–40.
- 890 Biesalski, Hans K. 2016. "Nutrition Meets the Microbiome: Micronutrients and the
891 Microbiota." *Annals of the New York Academy of Sciences* 1372 (1): 53–64.
- 892 Bowers, Robert M., Nikos C. Kyrpides, Ramunas Stepanauskas, Miranda Harmon-
893 Smith, Devin Doud, T. B. K. Reddy, Frederik Schulz, et al. 2017. "Minimum
894 Information about a Single Amplified Genome (MISAG) and a Metagenome-
895 Assembled Genome (MIMAG) of Bacteria and Archaea." *Nature Biotechnology* 35
896 (8): 725–31.
- 897 Campbell, James H., Patrick O'Donoghue, Alisha G. Campbell, Patrick Schwientek,

- 898 Alexander Sczyrba, Tanja Woyke, Dieter Söll, and Mircea Podar. 2013. "UGA Is an
899 Additional Glycine Codon in Uncultured SR1 Bacteria from the Human Microbiota."
900 *Proceedings of the National Academy of Sciences of the United States of America*
901 110 (14): 5540–45.
- 902 Chaumeil, Pierre-Alain, Aaron J. Mussig, Philip Hugenholtz, and Donovan H. Parks.
903 2019. "GTDB-Tk: A Toolkit to Classify Genomes with the Genome Taxonomy
904 Database." *Bioinformatics*, November.
905 <https://doi.org/10.1093/bioinformatics/btz848>.
- 906 Chen, Lin-Xing, Karthik Anantharaman, Alon Shaiber, A. Murat Eren, and Jillian F.
907 Banfield. 2020. "Accurate and Complete Genomes from Metagenomes." *Genome*
908 *Research* 30 (3): 315–33.
- 909 Chien, Hsiang-Lin, Hui-Yu Huang, and Cheng-Chun Chou. 2006. "Transformation of
910 Isoflavone Phytoestrogens during the Fermentation of Soymilk with Lactic Acid
911 Bacteria and Bifidobacteria." *Food Microbiology* 23 (8): 772–78.
- 912 Chow, Janet, Haiqing Tang, and Sarkis K. Mazmanian. 2011. "Pathobionts of the
913 Gastrointestinal Microbiota and Inflammatory Disease." *Current Opinion in*
914 *Immunology* 23 (4): 473–80.
- 915 Clooney, Adam G., Julia Eckenberger, Emilio Laserna-Mendieta, Kathryn A. Sexton,
916 Matthew T. Bernstein, Kathy Vagianos, Michael Sargent, et al. 2021. "Ranking
917 Microbiome Variance in Inflammatory Bowel Disease: A Large Longitudinal
918 Intercontinental Study." *Gut* 70 (3): 499–510.
- 919 Costello, Elizabeth K., Keaton Stagaman, Les Dethlefsen, Brendan J. M. Bohannan,
920 and David A. Relman. 2012. "The Application of Ecological Theory toward an
921 Understanding of the Human Microbiome." *Science* 336 (6086): 1255–62.
- 922 D'Aimmo, M. R., P. Mattarelli, B. Biavati, N. G. Carlsson, and T. Andlid. 2012. "The
923 Potential of Bifidobacteria as a Source of Natural Folate." *Journal of Applied*
924 *Microbiology* 112 (5): 975–84.
- 925 David, Lawrence A., Arne C. Materna, Jonathan Friedman, Maria I. Campos-Baptista,
926 Matthew C. Blackburn, Allison Perrotta, Susan E. Erdman, and Eric J. Alm. 2014.
927 "Host Lifestyle Affects Human Microbiota on Daily Timescales." *Genome Biology* 15
928 (7): R89.
- 929 Delmont, Tom O., and A. Murat Eren. 2016. "Identifying Contamination with Advanced
930 Visualization and Analysis Practices: Metagenomic Approaches for Eukaryotic
931 Genome Assemblies." *PeerJ* 4 (March): e1839.
- 932 Delmont, Tom O., Christopher Quince, Alon Shaiber, Özcan C. Esen, Sonny Tm Lee,
933 Michael S. Rappé, Sandra L. McLellan, Sebastian Lückner, and A. Murat Eren.
934 2018. "Nitrogen-Fixing Populations of Planctomycetes and Proteobacteria Are
935 Abundant in Surface Ocean Metagenomes." *Nature Microbiology* 3 (7): 804–13.
- 936 Denef, Vincent J. 2019. "Peering into the Genetic Makeup of Natural Microbial
937 Populations Using Metagenomics." In *Population Genomics: Microorganisms*,
938 edited by Martin F. Polz and Om P. Rajora, 49–75. Cham: Springer International
939 Publishing.
- 940 De Preter, Vicky, Veerle Bulteel, Peter Suenart, Karen Paula Geboes, Gert De
941 Hertogh, Anja Luypaerts, Karel Geboes, Kristin Verbeke, and Paul Rutgeerts. 2009.
942 "Pouchitis, Similar to Active Ulcerative Colitis, Is Associated with Impaired Butyrate
943 Oxidation by Intestinal Mucosa." *Inflammatory Bowel Diseases* 15 (3): 335–40.

- 944 D'Souza, Glen, Shraddha Shitut, Daniel Preussger, Ghada Yousif, Silvio Waschina, and
945 Christian Kost. 2018. "Ecology and Evolution of Metabolic Cross-Feeding
946 Interactions in Bacteria." *Natural Product Reports* 35 (5): 455–88.
- 947 Durack, Juliana, and Susan V. Lynch. 2019. "The Gut Microbiome: Relationships with
948 Disease and Opportunities for Therapy." *The Journal of Experimental Medicine* 216
949 (1): 20–40.
- 950 Eddy, Sean R. 2011. "Accelerated Profile HMM Searches." *PLoS Computational
951 Biology* 7 (10): e1002195.
- 952 Edgar, Robert C. 2004. "MUSCLE: Multiple Sequence Alignment with High Accuracy
953 and High Throughput." *Nucleic Acids Research* 32 (5): 1792–97.
- 954 Eiseman, B., W. Silen, G. S. Bascom, and A. J. Kauvar. 1958. "Fecal Enema as an
955 Adjunct in the Treatment of Pseudomembranous Enterocolitis." *Surgery* 44 (5):
956 854–59.
- 957 Eisenstein, Michael. 2020. "The Hunt for a Healthy Microbiome." *Nature* 577 (7792):
958 S6–8.
- 959 Enright, A. J., S. Van Dongen, and C. A. Ouzounis. 2002. "An Efficient Algorithm for
960 Large-Scale Detection of Protein Families." *Nucleic Acids Research* 30 (7): 1575–
961 84.
- 962 Eren, A. Murat, Özcan C. Esen, Christopher Quince, Joseph H. Vineis, Hilary G.
963 Morrison, Mitchell L. Sogin, and Tom O. Delmont. 2015. "Anvi'o: An Advanced
964 Analysis and Visualization Platform for 'Omics Data." *PeerJ* 3 (October): e1319.
- 965 Eren, A. Murat, Evan Kiefl, Alon Shaiber, Iva Veseli, Samuel E. Miller, Matthew S.
966 Schechter, Isaac Fink, et al. 2021. "Community-Led, Integrated, Reproducible
967 Multi-Omics with Anvi'o." *Nature Microbiology* 6 (1): 3–6.
- 968 Eren, A. Murat, Joseph H. Vineis, Hilary G. Morrison, and Mitchell L. Sogin. 2013. "A
969 Filtering Method to Generate High Quality Short Reads Using Illumina Paired-End
970 Technology." *PloS One* 8 (6): e66643.
- 971 Feng, Lihui, Arjun S. Raman, Matthew C. Hibberd, Jiye Cheng, Nicholas W. Griffin,
972 Yangqing Peng, Semen A. Leyn, Dmitry A. Rodionov, Andrei L. Osterman, and
973 Jeffrey I. Gordon. 2020. "Identifying Determinants of Bacterial Fitness in a Model of
974 Human Gut Microbial Succession." *Proceedings of the National Academy of
975 Sciences of the United States of America* 117 (5): 2622–33.
- 976 Finucane, Mariel M., Thomas J. Sharpton, Timothy J. Laurent, and Katherine S. Pollard.
977 2014. "A Taxonomic Signature of Obesity in the Microbiome? Getting to the Guts of
978 the Matter." *PloS One* 9 (1): e84689.
- 979 Galperin, Michael Y., Yuri I. Wolf, Kira S. Makarova, Roberto Vera Alvarez, David
980 Landsman, and Eugene V. Koonin. 2021. "COG Database Update: Focus on
981 Microbial Diversity, Model Organisms, and Widespread Pathogens." *Nucleic Acids
982 Research* 49 (D1): D274–81.
- 983 Gomes, Ana M. P., and F. Xavier Malcata. 1999. "Bifidobacterium Spp. and
984 Lactobacillus Acidophilus: Biological, Biochemical, Technological and Therapeutical
985 Properties Relevant for Use as Probiotics." *Trends in Food Science & Technology*
986 10 (4): 139–57.
- 987 Grehan, Martin J., Thomas Julius Borody, Sharyn M. Leis, Jordana Campbell, Hazel
988 Mitchell, and Antony Wettstein. 2010. "Durable Alteration of the Colonic Microbiota
989 by the Administration of Donor Fecal Flora." *Journal of Clinical Gastroenterology* 44

- 990 (8): 551–61.
- 991 Herrmann, Klaus M., and Lisa M. Weaver. 1999. "THE SHIKIMATE PATHWAY." *Annual*
992 *Review of Plant Physiology and Plant Molecular Biology* 50 (June): 473–503.
- 993 Human Microbiome Project Consortium. 2012. "Structure, Function and Diversity of the
994 Healthy Human Microbiome." *Nature* 486 (7402): 207–14.
- 995 Hyatt, Doug, Gwo-Liang Chen, Philip F. Locascio, Miriam L. Land, Frank W. Larimer,
996 and Loren J. Hauser. 2010. "Prodigal: Prokaryotic Gene Recognition and
997 Translation Initiation Site Identification." *BMC Bioinformatics* 11 (March): 119.
- 998 Isaac, Sandrine, Jose U. Scher, Ana Djukovic, Nuria Jiménez, Dan R. Littman, Steven
999 B. Abramson, Eric G. Pamer, and Carles Ubeda. 2017. "Short- and Long-Term
1000 Effects of Oral Vancomycin on the Human Intestinal Microbiota." *The Journal of*
1001 *Antimicrobial Chemotherapy* 72 (1): 128–36.
- 1002 Joossens, Marie, Geert Huys, Margo Cnockaert, Vicky De Preter, Kristin Verbeke, Paul
1003 Rutgeerts, Peter Vandamme, and Severine Vermeire. 2011. "Dysbiosis of the
1004 Faecal Microbiota in Patients with Crohn's Disease and Their Unaffected
1005 Relatives." *Gut* 60 (5): 631–37.
- 1006 Jungersen, Mikkel, Anette Wind, Eric Johansen, Jeffrey E. Christensen, Birgitte Stuer-
1007 Lauridsen, and Dorte Eskesen. 2014. "The Science behind the Probiotic Strain
1008 Bifidobacterium Animalis Subsp. Lactis BB-12(®)." *Microorganisms* 2 (2): 92–110.
- 1009 Kanehisa, M., and S. Goto. 2000. "KEGG: Kyoto Encyclopedia of Genes and
1010 Genomes." *Nucleic Acids Research* 28 (1): 27–30.
- 1011 Kanehisa, Minoru, Miho Furumichi, Mao Tanabe, Yoko Sato, and Kanae Morishima.
1012 2017. "KEGG: New Perspectives on Genomes, Pathways, Diseases and Drugs."
1013 *Nucleic Acids Research* 45 (D1): D353–61.
- 1014 Kanehisa, Minoru, Susumu Goto, Yoko Sato, Masayuki Kawashima, Miho Furumichi,
1015 and Mao Tanabe. 2014. "Data, Information, Knowledge and Principle: Back to
1016 Metabolism in KEGG." *Nucleic Acids Research* 42 (Database issue): D199–205.
- 1017 Kao, Dina, Brandi Roach, Marisela Silva, Paul Beck, Kevin Rioux, Gilaad G. Kaplan,
1018 Hsiu-Ju Chang, et al. 2017. "Effect of Oral Capsule- vs Colonoscopy-Delivered
1019 Fecal Microbiota Transplantation on Recurrent Clostridium Difficile Infection: A
1020 Randomized Clinical Trial." *JAMA: The Journal of the American Medical*
1021 *Association* 318 (20): 1985–93.
- 1022 Khoruts, Alexander, Johan Dicksved, Janet K. Jansson, and Michael J. Sadowsky.
1023 2010. "Changes in the Composition of the Human Fecal Microbiome after
1024 Bacteriotherapy for Recurrent Clostridium Difficile-Associated Diarrhea." *Journal of*
1025 *Clinical Gastroenterology* 44 (5): 354–60.
- 1026 Kirchhelle, Claas. 2018. "Pharming Animals: A Global History of Antibiotics in Food
1027 Production (1935–2017)." *Palgrave Communications* 4 (1): 96.
- 1028 Kleerebezem, Michiel, and Elaine E. Vaughan. 2009. "Probiotic and Gut Lactobacilli and
1029 Bifidobacteria: Molecular Approaches to Study Diversity and Activity." *Annual*
1030 *Review of Microbiology* 63: 269–90.
- 1031 Koenig, Jeremy E., Aymé Spor, Nicholas Scalfone, Ashwana D. Fricker, Jesse
1032 Stombaugh, Rob Knight, Lergus T. Angenent, and Ruth E. Ley. 2011. "Succession
1033 of Microbial Consortia in the Developing Infant Gut Microbiome." *Proceedings of*
1034 *the National Academy of Sciences of the United States of America* 108 Suppl 1
1035 (March): 4578–85.

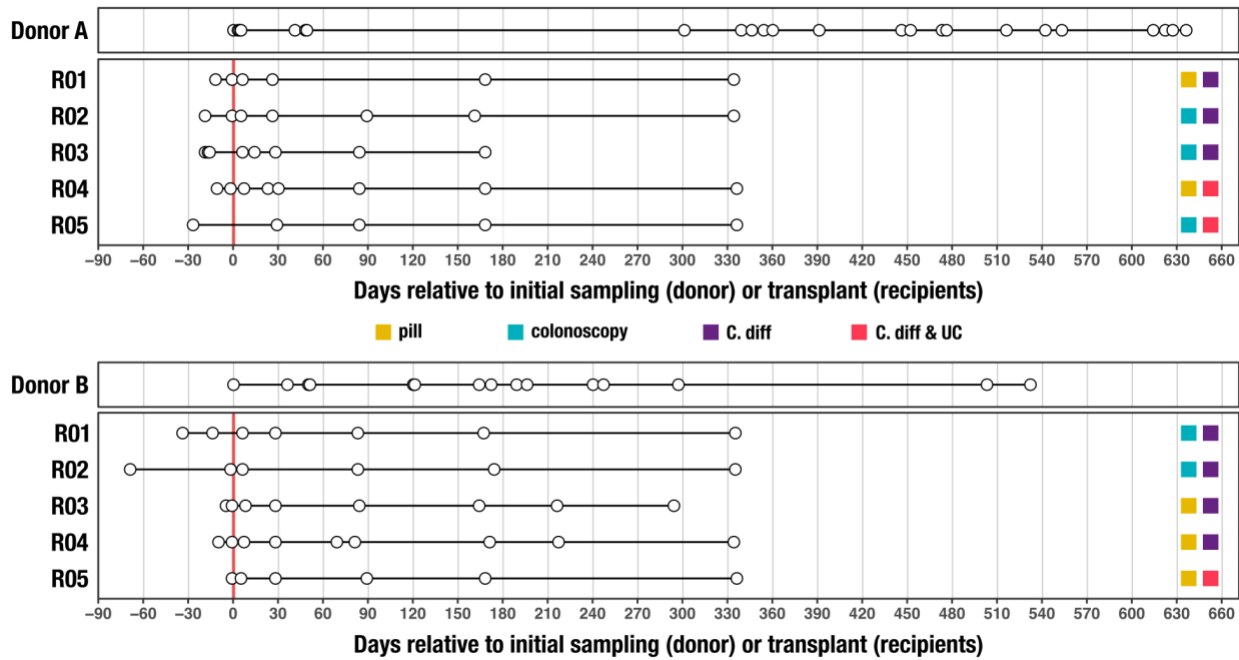
- 1036 Kolmogorov, Mikhail, Mikhail Rayko, Jeffrey Yuan, Evgeny Pevnikov, and Pavel
1037 Pevzner. 2019. "metaFlye: Scalable Long-Read Metagenome Assembly Using
1038 Repeat Graphs." *bioRxiv*, 637637.
- 1039 Köster, Johannes, and Sven Rahmann. 2012. "Snakemake—a Scalable Bioinformatics
1040 Workflow Engine." *Bioinformatics* 28 (19): 2520–22.
- 1041 Kowarsky, Mark, Joan Camunas-Soler, Michael Kertesz, Iwijn De Vlamincx, Winston
1042 Koh, Wenying Pan, Lance Martin, et al. 2017. "Numerous Uncharacterized and
1043 Highly Divergent Microbes Which Colonize Humans Are Revealed by Circulating
1044 Cell-Free DNA." *Proceedings of the National Academy of Sciences of the United
1045 States of America*, August. <https://doi.org/10.1073/pnas.1707009114>.
- 1046 Langmead, Ben, and Steven L. Salzberg. 2012. "Fast Gapped-Read Alignment with
1047 Bowtie 2." *Nature Methods* 9 (4): 357–59.
- 1048 Lee, S. Melanie, Gregory P. Donaldson, Zbigniew Mikulski, Silva Boyajian, Klaus Ley,
1049 and Sarkis K. Mazmanian. 2013. "Bacterial Colonization Factors Control Specificity
1050 and Stability of the Gut Microbiota." *Nature* 501 (7467): 426–29.
- 1051 Lee, Sonny T. M., Stacy A. Kahn, Tom O. Delmont, Alon Shaiber, Özcan C. Esen,
1052 Nathaniel A. Hubert, Hilary G. Morrison, Dionysios A. Antonopoulos, David T.
1053 Rubin, and A. Murat Eren. 2017. "Tracking Microbial Colonization in Fecal
1054 Microbiota Transplantation Experiments via Genome-Resolved Metagenomics."
1055 *Microbiome* 5 (1): 50.
- 1056 Ley, Ruth E., Peter J. Turnbaugh, Samuel Klein, and Jeffrey I. Gordon. 2006. "Microbial
1057 Ecology: Human Gut Microbes Associated with Obesity." *Nature* 444 (7122): 1022–
1058 23.
- 1059 Li, Heng, Bob Handsaker, Alec Wysoker, Tim Fennell, Jue Ruan, Nils Homer, Gabor
1060 Marth, Goncalo Abecasis, Richard Durbin, and 1000 Genome Project Data
1061 Processing Subgroup. 2009. "The Sequence Alignment/Map Format and
1062 SAMtools." *Bioinformatics* 25 (16): 2078–79.
- 1063 Lloyd-Price, Jason, Galeb Abu-Ali, and Curtis Huttenhower. 2016. "The Healthy Human
1064 Microbiome." *Genome Medicine* 8 (1): 51.
- 1065 Lloyd-Price, Jason, Cesar Arze, Ashwin N. Ananthakrishnan, Melanie Schirmer, Julian
1066 Avila-Pacheco, Tiffany W. Poon, Elizabeth Andrews, et al. 2019. "Multi-Omics of
1067 the Gut Microbial Ecosystem in Inflammatory Bowel Diseases." *Nature* 569 (7758):
1068 655–62.
- 1069 Lynch, Susan V., and Oluf Pedersen. 2016. "The Human Intestinal Microbiome in
1070 Health and Disease." *The New England Journal of Medicine* 375 (24): 2369–79.
- 1071 Maignien, Loïs, Emelia A. DeForce, Meghan E. Chafee, A. Murat Eren, and Sheri L.
1072 Simmons. 2014. "Ecological Succession and Stochastic Variation in the Assembly
1073 of Arabidopsis Thaliana Phyllosphere Communities." *mBio* 5 (1): e00682–13.
- 1074 Martens, J. H., H. Barg, M. J. Warren, and D. Jahn. 2002. "Microbial Production of
1075 Vitamin B12." *Applied Microbiology and Biotechnology* 58 (3): 275–85.
- 1076 Martiny, Adam C., Kathleen Treseder, and Gordon Pusch. 2013. "Phylogenetic
1077 Conservatism of Functional Traits in Microorganisms." *The ISME Journal* 7 (4):
1078 830–38.
- 1079 McBurney, Michael I., Cindy Davis, Claire M. Fraser, Barbara O. Schneeman, Curtis
1080 Huttenhower, Kristin Verbeke, Jens Walter, and Marie E. Latulippe. 2019.
1081 "Establishing What Constitutes a Healthy Human Gut Microbiome: State of the

- 1082 Science, Regulatory Considerations, and Future Directions.” *The Journal of*
1083 *Nutrition* 149 (11): 1882–95.
- 1084 Messer, J. S., E. R. Liechty, O. A. Vogel, and E. B. Chang. 2017. “Evolutionary and
1085 Ecological Forces That Shape the Bacterial Communities of the Human Gut.”
1086 *Mucosal Immunology* 10 (3): 567–79.
- 1087 Minoche, André E., Juliane C. Dohm, and Heinz Himmelbauer. 2011. “Evaluation of
1088 Genomic High-Throughput Sequencing Data Generated on Illumina HiSeq and
1089 Genome Analyzer Systems.” *Genome Biology* 12 (11): R112.
- 1090 Ott, S. J., M. Musfeldt, D. F. Wenderoth, J. Hampe, O. Brant, U. R. Fölsch, K. N.
1091 Timmis, and S. Schreiber. 2004. “Reduction in Diversity of the Colonic Mucosa
1092 Associated Bacterial Microflora in Patients with Active Inflammatory Bowel
1093 Disease.” *Gut* 53 (5): 685–93.
- 1094 Parks, Donovan H., Maria Chuvochina, David W. Waite, Christian Rinke, Adam
1095 Skarszewski, Pierre-Alain Chaumeil, and Philip Hugenholtz. 2018. “A Standardized
1096 Bacterial Taxonomy Based on Genome Phylogeny Substantially Revises the Tree
1097 of Life.” *Nature Biotechnology* 36 (10): 996–1004.
- 1098 Pasolli, Edoardo, Francesco Asnicar, Serena Manara, Moreno Zolfo, Nicolai Karcher,
1099 Federica Armanini, Francesco Beghini, et al. 2019. “Extensive Unexplored Human
1100 Microbiome Diversity Revealed by Over 150,000 Genomes from Metagenomes
1101 Spanning Age, Geography, and Lifestyle.” *Cell* 176 (3): 649–62.e20.
- 1102 Peng, Yu, Henry C. M. Leung, S. M. Yiu, and Francis Y. L. Chin. 2012. “IDBA-UD: A de
1103 Novo Assembler for Single-Cell and Metagenomic Sequencing Data with Highly
1104 Uneven Depth.” *Bioinformatics* 28 (11): 1420–28.
- 1105 Philippot, Laurent, Siv G. E. Andersson, Tom J. Battin, James I. Prosser, Joshua P.
1106 Schimel, William B. Whitman, and Sara Hallin. 2010. “The Ecological Coherence of
1107 High Bacterial Taxonomic Ranks.” *Nature Reviews. Microbiology* 8 (7): 523–29.
- 1108 Plichta, Damian R., Daniel B. Graham, Sathish Subramanian, and Ramnik J. Xavier.
1109 2019. “Therapeutic Opportunities in Inflammatory Bowel Disease: Mechanistic
1110 Dissection of Host-Microbiome Relationships.” *Cell* 178 (5): 1041–56.
- 1111 Podlesny, Daniel, and W. Florian Fricke. 2020. “Microbial Strain Engraftment,
1112 Persistence and Replacement after Fecal Microbiota Transplantation.” *medRxiv*,
1113 September, 2020.09.29.20203638.
- 1114 Pompei, Anna, Lisa Cordisco, Alberto Amaretti, Simona Zanoni, Diego Matteuzzi, and
1115 Maddalena Rossi. 2007. “Folate Production by Bifidobacteria as a Potential
1116 Probiotic Property.” *Applied and Environmental Microbiology* 73 (1): 179–85.
- 1117 Price, Morgan N., Paramvir S. Dehal, and Adam P. Arkin. 2010. “FastTree 2--
1118 Approximately Maximum-Likelihood Trees for Large Alignments.” *PloS One* 5 (3):
1119 e9490.
- 1120 Pritchard, Leighton, Rachel H. Glover, Sonia Humphris, John G. Elphinstone, and Ian K.
1121 Toth. 2016. “Genomics and Taxonomy in Diagnostics for Food Security: Soft-
1122 Rotting Enterobacterial Plant Pathogens.” *Analytical Methods* 8 (1): 12–24.
- 1123 Quince, Christopher, Tom O. Delmont, Sébastien Raguideau, Johannes Alneberg,
1124 Aaron E. Darling, Gavin Collins, and A. Murat Eren. 2017. “DESMAN: A New Tool
1125 for de Novo Extraction of Strains from Metagenomes.” *Genome Biology* 18 (1): 181.
- 1126 Rinke, Christian, Patrick Schwientek, Alexander Sczyrba, Natalia N. Ivanova, Iain J.
1127 Anderson, Jan-Fang Cheng, Aaron Darling, et al. 2013. “Insights into the

- 1128 Phylogeny and Coding Potential of Microbial Dark Matter.” *Nature* 499 (7459): 431–
1129 37.
- 1130 Rothschild, Daphna, Omer Weissbrod, Elad Barkan, Alexander Kurilshikov, Tal Korem,
1131 David Zeevi, Paul I. Costea, et al. 2018. “Environment Dominates over Host
1132 Genetics in Shaping Human Gut Microbiota.” *Nature* 555 (7695): 210–15.
- 1133 Schell, Mark A., Maria Karmirantzou, Berend Snel, David Vilanova, Bernard Berger,
1134 Gabriella Pessi, Marie-Camille Zwahlen, et al. 2002. “The Genome Sequence of
1135 *Bifidobacterium Longum* Reflects Its Adaptation to the Human Gastrointestinal
1136 Tract.” *Proceedings of the National Academy of Sciences of the United States of*
1137 *America* 99 (22): 14422–27.
- 1138 Schirmer, Melanie, Ashley Garner, Hera Vlamakis, and Ramnik J. Xavier. 2019.
1139 “Microbial Genes and Pathways in Inflammatory Bowel Disease.” *Nature Reviews.*
1140 *Microbiology* 17 (8): 497–511.
- 1141 Schmidt, Thomas S. B., Jeroen Raes, and Peer Bork. 2018. “The Human Gut
1142 Microbiome: From Association to Modulation.” *Cell* 172 (6): 1198–1215.
- 1143 Shahinas, Dea, Michael Silverman, Taylor Sittler, Charles Chiu, Peter Kim, Emma
1144 Allen-Vercoe, Scott Weese, Andrew Wong, Donald E. Low, and Dylan R. Pillai.
1145 2012. “Toward an Understanding of Changes in Diversity Associated with Fecal
1146 Microbiome Transplantation Based on 16S rRNA Gene Deep Sequencing.” *mBio* 3
1147 (5): e00338–12.
- 1148 Shaiber, Alon, Amy D. Willis, Tom O. Delmont, Simon Roux, Lin-Xing Chen, Abigail C.
1149 Schmid, Mahmoud Yousef, et al. 2020. “Functional and Genetic Markers of Niche
1150 Partitioning among Enigmatic Members of the Human Oral Microbiome.” *Genome*
1151 *Biology* 21 (1): 292.
- 1152 Sharon, Itai, Michael J. Morowitz, Brian C. Thomas, Elizabeth K. Costello, David A.
1153 Relman, and Jillian F. Banfield. 2013. “Time Series Community Genomics Analysis
1154 Reveals Rapid Shifts in Bacterial Species, Strains, and Phage during Infant Gut
1155 Colonization.” *Genome Research* 23 (1): 111–20.
- 1156 Sheth, Ravi U., Mingqiang Li, Weiqian Jiang, Peter A. Sims, Kam W. Leong, and Harris
1157 H. Wang. 2019. “Spatial Metagenomic Characterization of Microbial Biogeography
1158 in the Gut.” *Nature Biotechnology* 37 (8): 877–83.
- 1159 Smillie, Christopher S., Jenny Sauk, Dirk Gevers, Jonathan Friedman, Jaeyun Sung,
1160 Ilan Youngster, Elizabeth L. Hohmann, et al. 2018. “Strain Tracking Reveals the
1161 Determinants of Bacterial Engraftment in the Human Gut Following Fecal
1162 Microbiota Transplantation.” *Cell Host & Microbe* 23 (2): 229–40.e5.
- 1163 Sokol, Harry, and Philippe Seksik. 2010. “The Intestinal Microbiota in Inflammatory
1164 Bowel Diseases: Time to Connect with the Host.” *Current Opinion in*
1165 *Gastroenterology* 26 (4): 327–31.
- 1166 Strozzi, G. Paolo, and Luca Mogna. 2008. “Quantification of Folic Acid in Human Feces
1167 after Administration of *Bifidobacterium* Probiotic Strains.” *Journal of Clinical*
1168 *Gastroenterology* 42 Suppl 3 Pt 2 (September): S179–84.
- 1169 Sugahara, Hirosuke, Toshitaka Odamaki, Nanami Hashikura, Fumiaki Abe, and Jin-
1170 Zhong Xiao. 2015. “Differences in Folate Production by *Bifidobacteria* of Different
1171 Origins.” *Bioscience of Microbiota, Food and Health* 34 (4): 87–93.
- 1172 Swidsinski, Alexander, Jutta Weber, Vera Loening-Baucke, Laura P. Hale, and Herbert
1173 Lochs. 2005. “Spatial Organization and Composition of the Mucosal Flora in

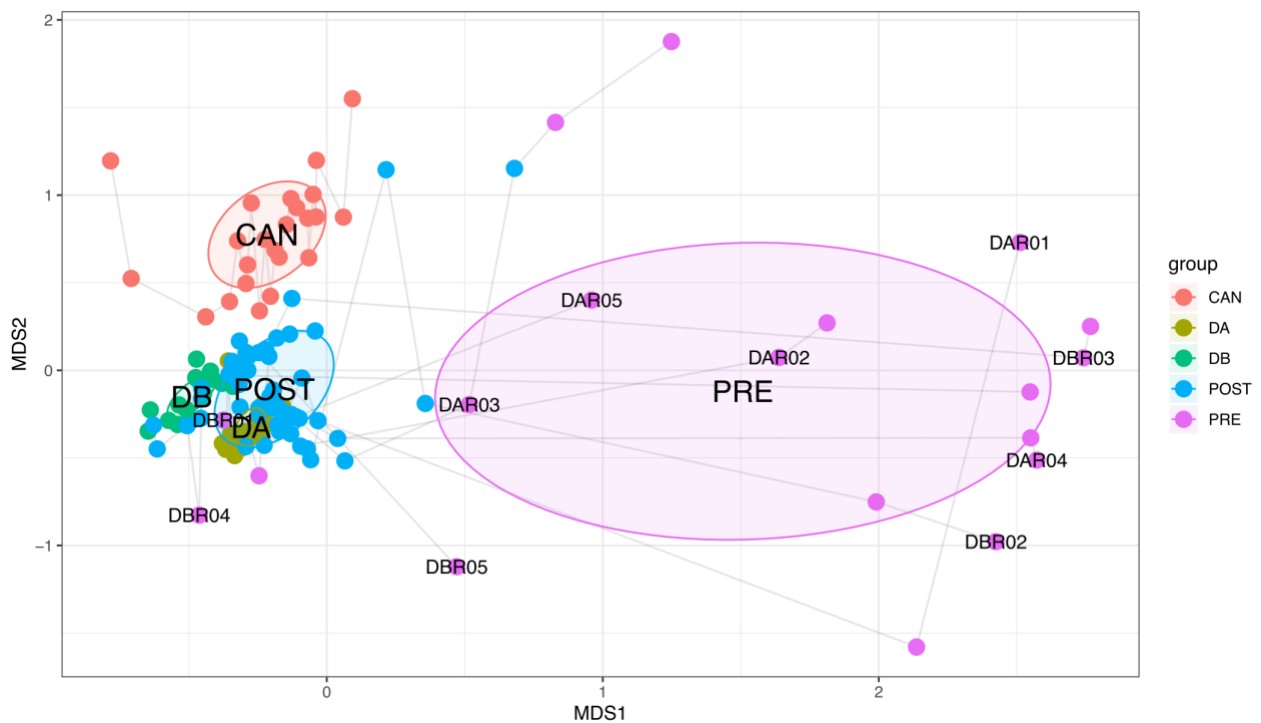
- 1174 Patients with Inflammatory Bowel Disease.” *Journal of Clinical Microbiology* 43 (7):
1175 3380–89.
- 1176 Tatusov, Roman L., Natalie D. Fedorova, John D. Jackson, Aviva R. Jacobs, Boris
1177 Kiryutin, Eugene V. Koonin, Dmitri M. Krylov, et al. 2003. “The COG Database: An
1178 Updated Version Includes Eukaryotes.” *BMC Bioinformatics* 4 (September): 41.
- 1179 Utter, Daniel R., Gary G. Borisy, A. Murat Eren, Colleen M. Cavanaugh, and Jessica L.
1180 Mark Welch. 2020. “Metapangenomics of the Oral Microbiome Provides Insights
1181 into Habitat Adaptation and Cultivar Diversity.” *Genome Biology* 21 (1): 293.
- 1182 Vanni, Chiara, Matthew S. Schechter, Silvia G. Acinas, Albert Barberán, Pier Luigi
1183 Buttigieg, Emilio O. Casamayor, Tom O. Delmont, et al. 2020. “Unifying the Global
1184 Coding Sequence Space Enables the Study of Genes with Unknown Function
1185 across Biomes.” *Cold Spring Harbor Laboratory*.
1186 <https://doi.org/10.1101/2020.06.30.180448>.
- 1187 Ventura, Marco, Sarah O’Flaherty, Marcus J. Claesson, Francesca Turrone, Todd R.
1188 Klaenhammer, Douwe van Sinderen, and Paul W. O’Toole. 2009. “Genome-Scale
1189 Analyses of Health-Promoting Bacteria: Probiogenomics.” *Nature Reviews*.
1190 *Microbiology* 7 (1): 61–71.
- 1191 Vineis, Joseph H., Daina L. Ringus, Hilary G. Morrison, Tom O. Delmont, Sushila Dalal,
1192 Laura H. Raffals, Dionysios A. Antonopoulos, et al. 2016. “Patient-Specific
1193 *Bacteroides* Genome Variants in Pouchitis.” *mBio* 7 (6): e01713–16,
1194 [/mbio/7/6/e01713–16.atom](https://doi.org/10.1128/mBio.01713-16).
- 1195 Walker, Bruce J., Thomas Abeel, Terrance Shea, Margaret Priest, Amr Abouelliel,
1196 Sharadha Sakthikumar, Christina A. Cuomo, et al. 2014. “Pilon: An Integrated Tool
1197 for Comprehensive Microbial Variant Detection and Genome Assembly
1198 Improvement.” *PLoS One* 9 (11): e112963.
- 1199 Walter, Jens, Anissa M. Armet, B. Brett Finlay, and Fergus Shanahan. 2020.
1200 “Establishing or Exaggerating Causality for the Gut Microbiome: Lessons from
1201 Human Microbiota-Associated Rodents.” *Cell* 180 (2): 221–32.
- 1202 Wexler, Aaron G., and Andrew L. Goodman. 2017. “An Insider’s Perspective:
1203 *Bacteroides* as a Window into the Microbiome.” *Nature Microbiology*.
1204 <https://doi.org/10.1038/nmicrobiol.2017.26>.
- 1205 Wood, Derrick E., Jennifer Lu, and Ben Langmead. 2019. “Improved Metagenomic
1206 Analysis with Kraken 2.” *Genome Biology* 20 (1): 257.
- 1207 Wu, Guojun, Naisi Zhao, Chenhong Zhang, Yan Y. Lam, and Liping Zhao. 2021. “Guild-
1208 Based Analysis for Understanding Gut Microbiome in Human Health and
1209 Diseases.” *Genome Medicine* 13 (1): 22.
- 1210 Yasuda, Koji, Keunyoung Oh, Boyu Ren, Timothy L. Tickle, Eric A. Franzosa, Lynn M.
1211 Wachtman, Andrew D. Miller, et al. 2015. “Biogeography of the Intestinal Mucosal
1212 and Luminal Microbiome in the Rhesus Macaque.” *Cell Host & Microbe* 17 (3):
1213 385–91.

1214 Supplementary Figures



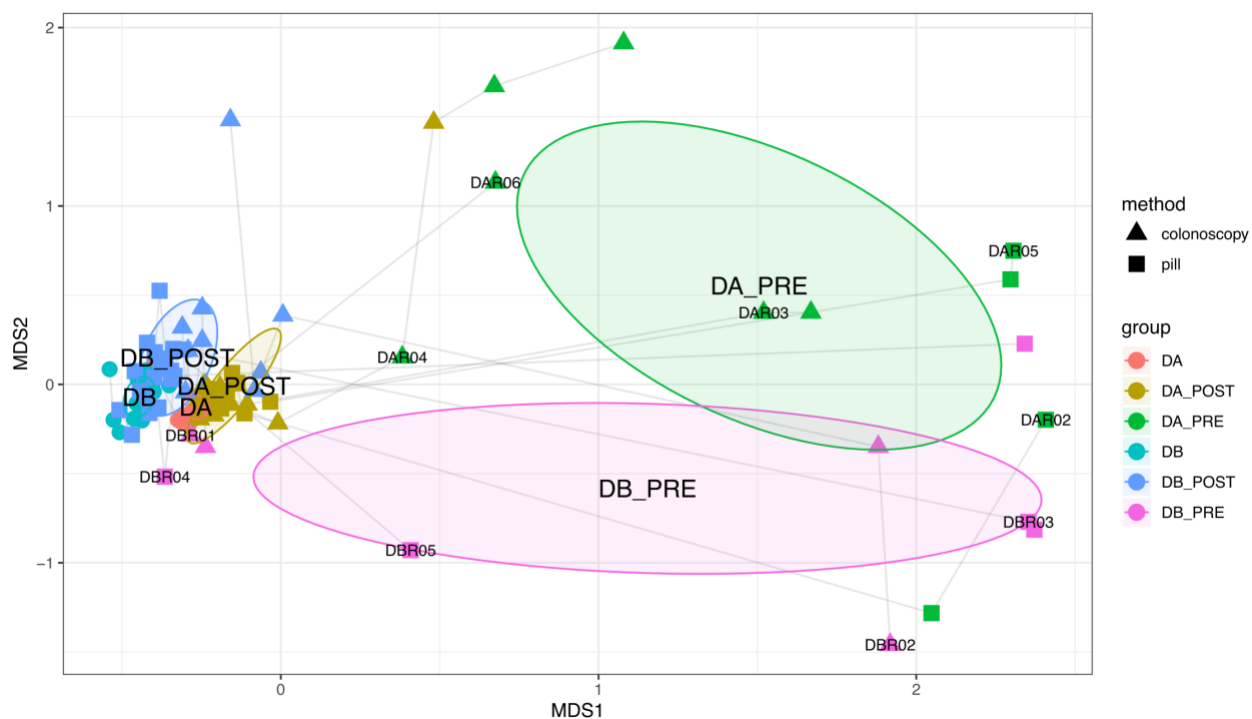
1215

1216 **Supplementary Figure 1. Timeline of stool samples collected from FMT study.** Each circle represents a stool
 1217 sample collected from either an FMT donor or FMT recipient. The thicker, red vertical line at day 0 represents the FMT
 1218 event for each recipient. FMT method (pill or colonoscopy) and FMT recipient health and disease state (C. diff - chronic
 1219 recurrent *Clostridium difficile* infection, UC - ulcerative colitis) are indicated on the right.

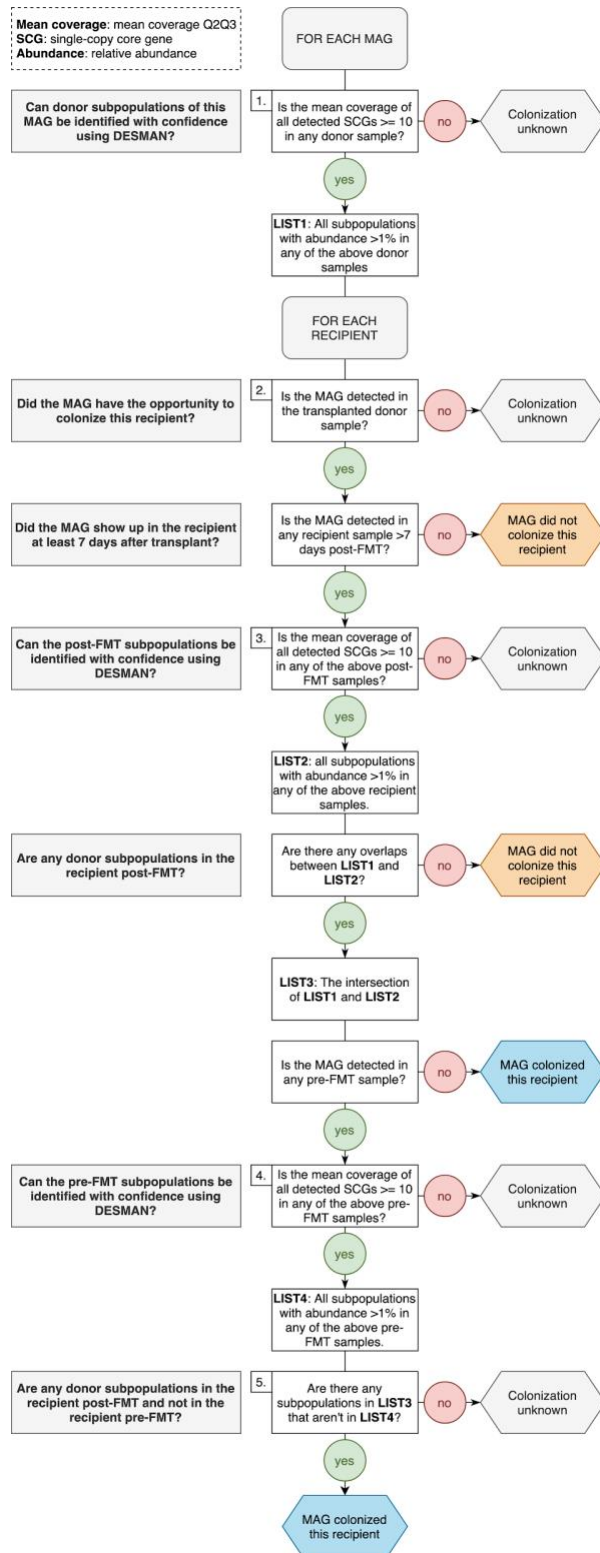


1220

1221 **Supplementary Figure 2. Nonmetric multidimensional scaling (NMDS) ordination of the taxonomic composition**
1222 **of donor, recipient, and Canadian gut metagenomes at the genus level based on Morisita-Horn dissimilarity.**
1223 Samples from the same participant are joined by lines with the earliest time point labeled. CAN: Canadian gut
1224 metagenomes, DA: donor A, DB: donor B, POST: recipients post-FMT, PRE: recipients pre-FMT.



1225 **Supplementary Figure 3. Nonmetric multidimensional scaling (NMDS) ordination of the taxonomic composition**
1226 **of the donor and recipient metagenomes at genus level based on Morisita-Horn dissimilarity.** Samples from the
1227 same participant are joined by lines with the earliest time point labeled. DA_POST: donor A recipients post-FMT,
1228 DA_PRE: donor A recipients pre-FMT, DA: donor A, DB_POST: donor B recipients post-FMT, DB_PRE: donor B
1229 recipients pre-FMT, DB: donor B.
1230



1231

1232 **Supplementary Figure 4.** A flowchart outlining our method to assign successful colonization, failed colonization, or
 1233 undetermined colonization phenotypes to donor-derived populations in the recipients of that donor's stool.

1234 Supplementary Tables ()

1235 **Supplementary Table 1: Description of FMT study and stool samples collected.** a) Description of FMT donor stool
1236 samples and SRA accession numbers. b) Description of FMT recipient samples and SRA accession numbers. c)
1237 Description of transplantation events.

1238 **Supplementary Table 2: Description of FMT metagenomes and co-assemblies.** a) Metagenome SRA accession
1239 numbers and number of metagenomic short-reads sequenced and mapped to co-assemblies and MAGs. b) Phylum
1240 level taxonomic composition of metagenomes. c) Genus level taxonomic composition of metagenomes. d) Summary
1241 statistics for contigs from metagenome co-assemblies.

1242 **Supplementary Table 3: Description of MAGs.** a) Summary statistics and taxonomic assignments for MAGs. b) and
1243 c) Detection of Donor A and Donor B MAGs in FMT metagenomes, respectively. d) and e) Detection of Donor A and
1244 Donor B MAGs in global gut metagenomes, respectively. f) and g) Detection summary statistics of Donor A and Donor
1245 B MAGs in global gut metagenomes, respectively.

1246 **Supplementary Table 4:** Accession numbers of gut metagenomes from 17 countries.

1247 **Supplementary Table 5: MAG subpopulation information.** a) and b) Number of Donor A and Donor B MAG
1248 subpopulations detected in FMT metagenomes, respectively. c) and d) Subpopulation composition of Donor A and
1249 Donor B MAGs in FMT metagenomes, respectively.

1250 **Supplementary Table 6:** MAG/recipient pair colonization outcomes and MAG mean coverage in the 2nd and 3rd
1251 quartiles in stool samples used for transplantation.

1252 **Supplementary Table 7: Description of high vs. low-fitness populations.** a) Taxonomic assignments and genome
1253 size estimates for high- and low-fitness populations. b) KEGG module completeness information for high- and low-
1254 fitness populations. c) Raw KEGG module enrichment information for high- and low-fitness populations. d) KEGG
1255 module enrichment and categorical information for the 33 modules enriched in high-fitness populations. e) and f)
1256 Completeness information for the 33 modules enriched in high-fitness populations in all high- and low-fitness
1257 populations.

1258 **Supplementary Table 8:** a) List of genomes from healthy individuals and individuals with IBD. b) Module completion
1259 values across genomes.

1260 **Supplementary Table 9: Bifidobacteria functional analysis.** a) Accession numbers for *Bifidobacteria* reference
1261 genomes. b) Summary statistics for *Bifidobacteria* MAGs and reference genomes. c) Prevalence of *Bifidobacteria*
1262 MAGs in global gut metagenomes. d) gANI percent identity between *Bifidobacteria* genomes. e) gANI percent alignment
1263 coverage between *Bifidobacteria* genomes. f) KOfams enriched in different *Bifidobacteria* species. g) KOfam presence
1264 and absence in *Bifidobacteria* genomes. h) COG functions enriched in different *Bifidobacteria* species. i) COG function
1265 presence and absence in *Bifidobacteria* genomes. j) KEGG modules enriched in different *Bifidobacteria* species. k)
1266 KEGG module completeness in *Bifidobacteria* genomes.